JOURNAL OF APPLIED PHYSICS

JOURNAL
OF
APPLIED PHYSICS

Vol. 16, No. 5 MAY, 1945

In This Issue

Page

Contributed Original Research

Mechanics of the Metal Cutting Process. I. Orthogonal Cutting and a Type 2 Chip M. EUGENE MERCHANT 267

Optimum Height of Flight of Winged Rocket- or Jet-Bomb M. ZBIGNIEW L. KRZYWOBLOCKI 275

Deflection Sensitivity of Parallel-Wire Lines in Cathode-Ray Oscillographs H. GUNTHER RUDENBERG 279

Novel Form of Refrigerator J. R. ROEBUCK 285

General Theory of Stresses and Displacements in Layered Soil Systems. III D. M. BURMISTER 296

Stability of Low Pressure Mercury Arcs as a Function of Current PAUL COPELAND AND W. H. SPARING 302

Validity of the Pole Figure BEULAH FIELD DECKER 309

Message to All Interested in Physics HOMER L. DODGE 310

Letter to the Editor:

Wave Equation for Finite Elastic Strains A. NADAI 313

In Every Issue

Here and There 311

New Booklets 311

New Books 312

Recent Applications of Physics 314

Index to Advertisers xxxii

BOARD OF EDITORS

ELMER HUTCHISSON, *Editor*

Associate Editors

R. B. BARNES
OTTO BEECK
W. F. BUSSE
S. H. CALDWELL
CLARK GOODMAN
SELIG HECHT
W. J. LYONS
MORRIS MUSKAT
THOMAS H. OSGOOD
PAUL E. SABINE
FREDERICK SEITZ
J. R. TOWNSEND

Publication of the American Institute of Physics

ADMINISTRATIVE STAFF

HENRY A. BARTON, *Director*

MADELINE M. MITCHELL, *Publications Manager*

JOHN T. TATE, *Adviser on Publications*

GOVERNING BOARD

PAUL E. KLOPSTEG, *Chairman*

WALLACE WATERFALL, *Secretary*

GEORGE B. PEGRAM, *Treasurer*

T. D. COPE
R. B. DOW
L. A. DUBRIDGE
FLOYD A. FIRESTONE
HARVEY FLETCHER
R. C. GIBBS
K. S. GIBSON
HERMANN MARK
A. G. WORTHING
JOHN T. TATE
L. W. TAYLOR
N. W. TAYLOR
WALLACE WATERFALL

The JOURNAL OF APPLIED PHYSICS, published monthly at Prince and Lemon Sts., Lancaster, Pa., is devoted to physics in its role as the science basic to other natural sciences and to the arts and industries. Previous to 1937 this publication was known as PHYSICS. The JOURNAL OF APPLIED PHYSICS publishes editorials, news of physicists, and reviews, as well as technical papers of applied physics.

Manuscripts should be submitted to Elmer Hutchisson, Editor Case School of Applied Science, Cleveland 6, Ohio.

Subscriptions and orders for back numbers should be addressed to Prince and Lemon Streets, Lancaster, Pa. or to the American Institute of Physics, 57 East 55 Street, New York 22, N. Y.

Subscription Price

	U. S. AND CANADA	ELSEWHERE
To members of scientific societies	$5.00	$5.70
To all others	7.00	7.70

Back Number Prices

Complete set: Vol. 1, July, 1931–Vol. 15, 1944—$94.50
Yearly back number rate: $7.70
Single copies: $0.70 each.

Changes of address and proofs should be addressed to the Publications Manager.

Advertising rates supplied on request. Orders, advertising copy, and cuts should be sent to the American Institute of Physics.

Entered as second class matter January 22, 1937, at the Post Office at Lancaster, Pennsylvania, under the Act of March 3, 1879
Accepted for mailing at the special rate of postage provided for in the Act of February 28, 1925, authorized May 2, 1932.

Copyright 1945, by the American Institute of Physics.

Journal
of
Applied Physics

Volume 16, Number 5 May, 1945

Contributed Original Research

Mechanics of the Metal Cutting Process. I. Orthogonal Cutting and a Type 2 Chip

M. Eugene Merchant
Research Department, The Cincinnati Milling Machine Company, Cincinnati, Ohio

(Received November 15, 1944)

An analysis of the chip geometry and the force system found in the case of orthogonal cutting accompanied by a type 2 chip has yielded a collection of useful equations which make possible the study of actual machining operations in terms of basic mechanical quantities. The shearing strain undergone by the metal during chip formation, and the velocities of shear and of chip flow are among the geometrical quantities which can be quantitatively determined. The force relationships permit calculation of such quantities as the various significant force components, stresses, the coefficient of friction between chip and cutting tool, and the work done in shearing the metal and in overcoming friction on the tool face. The experimental methods by which such analyses can be readily made are described. Observed and calculated values from typical tests are presented.

INTRODUCTION

THE process of the cutting or machining of metal is no doubt the most widely-used and versatile of any of the strictly mechanical processes employed in industry. In spite of this fact, it is not until recently that any more than the rudiments of the fundamental mechanics of this process have been known. However, in recent years progress in this direction has been more rapid.

A proper, quantitative understanding of the mechanics of any system makes possible the analysis of such a system in terms of basic physical quantities common to all of mechanics—forces, stresses and strains, velocities, energy distribution, etc. Such information is essential if the design and control of similar systems are to be handled on anything other than an empirical basis. For instance, an understanding of the mechanics of simple types of beam systems is an essential if the design and control of safe, economical machinery or buildings or bridges is to be effected by other than trial and error. Similarly, a knowledge of the mechanics of the system tool-chip-workpiece is very necessary to sound design and to efficient control of metal cutting tools, of the metal to be cut, and even of the machine tools behind these elements.

In this series of papers, to be contributed from time to time as the research progresses, it is the purpose of the writer to set forth certain original findings in regard to the mechanics and physics of the various aspects of the metal cutting process. While the discussions will be limited mainly to the cutting of metal, it will be evident that much of the theory is applicable to the cutting process in general.

ORTHOGONAL CUTTING AND THE TYPE 2 CHIP

The analysis presented in this paper is in theory limited to the case of orthogonal cutting

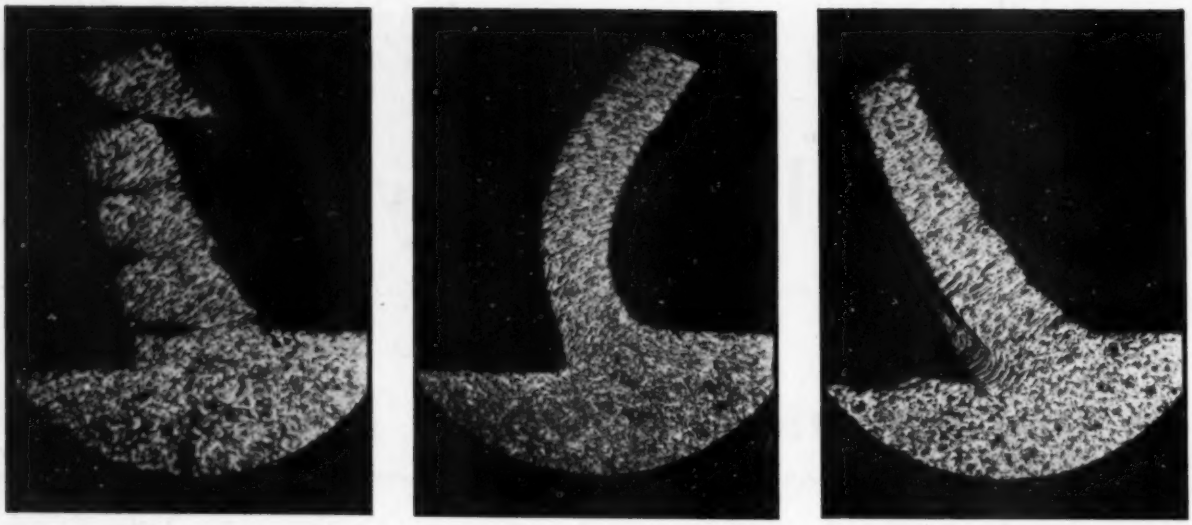

FIG. 1. The three basic chip types according to Ernst: Type 1, Discontinuous or segmental chip, Type 2, Continuous chip without built-up edge, and Type 3, Continuous chip with built-up edge.

with a tool having a plane face and a single straight cutting edge. The term "orthogonal cutting" has been coined[1] to cover the case where the cutting tool generates a plane surface parallel to an original plane surface of the material being cut and is set with its cutting edge perpendicular to the direction of relative motion of tool and workpiece. This is to distinguish it from the more general cases where the cutting edge is oblique to the direction of relative motion, termed oblique cutting, or where the surface generated is not a plane, to be discussed later in this series.

If in practice the above conditions are fulfilled to a good degree of approximation, then the present analysis also holds to a good degree of approximation. For instance, in a conventional turning operation with a single point tool there are at least two cutting edges; the first removes the major amount of material while the second produces the final surface. In addition the surfaces generated are not plane but cylindrical. Further, the cutting edge is often slightly oblique to the direction of relative motion of tool and work. However, if the depth of cut is quite large compared to the value of the feed per revolution, and if the tool has no appreciable nose radius, then the condition requiring a single straight cutting edge is well approximated. If the radius of the cylindrical surface generated is large compared to the thickness of the chip removed, then the approximation to a plane surface is good. If the primary cutting edge is not oblique by more than a few degrees, then the approximation to orthogonality is good. Some, if not all, of these factors will be treated in a quantitative manner later in this series.

As for the geometry of chip formation, it has been pointed out by Ernst[2] that there are three basic types of chips found in the cutting of metal, as illustrated in his classic examples given in Fig. 1. Type 1 is discontinuous, while types 2 and 3 are continuous. Type 3, however, has a so called "built-up edge" interposed between chip and tool in the vicinity of the cutting edge.

Strictly speaking, the analysis presented in this paper applies only to the type 2 chip. However, it has been found by experiment that it generally offers a good approximation in the case of the type 3 chip also.

When machining steel with the sintered-carbide type of tool materials, at recommended speeds, a type 2 chip is practically always produced, so that the present analysis is particularly apt for application to such operations. Fig. 2 is a photomicrograph of a type 2 chip obtained with a sintered-carbide tool having a negative rake angle and cutting SAE 1112 steel at 780 ft./min. The cutting tool is moving from right to left, as indicated by the arrow, and the chip is flowing upward relative to the tool.

[1] M. E. Merchant, J. App. Mech. **11**, A168–A175(1944).

[2] H. Ernst, "Physics of metal cutting," *Machining of Metals* (American Society for Metals, 1938), p. 24.

GEOMETRY OF FORMATION OF THE TYPE 2 CHIP

A. Theory

As may be seen from Figs. 1 and 2, the type 2 chip is formed by a process of shear which is approximately confined to a single plane extending from the cutting edge to the work surface ahead of the tool. This plane will be termed the "shear plane," and the angle which it makes with the surface generated will be designated by ϕ. This angle can vary over a fairly wide range, depending on the conditions existing during cutting.

The mechanism of chip formation by a process of shear such as described above can be illustrated by the successive displacement of cards in a stack, as shown in Fig. 3. Each successive card is displaced forward a small amount with respect to its neighbor as the cutting tool progresses. The crystal structure of the metal, represented by circles drawn on the sides of the stack of cards, is elongated by the process of shear, the direction of elongation coinciding with the direction of the major axes of the ellipses produced in Fig. 3. It is evident that the direction of crystal elongation is considerably different from the direction of shear, making an angle ψ with the latter direction. Returning to Fig. 2, it may be seen that this situation is confirmed by the actual chip photomicrograph. The elongated crystal structure in the chip is seen to originate at the shear plane, the elongated grains in the vicinity of this plane meeting it at a definite

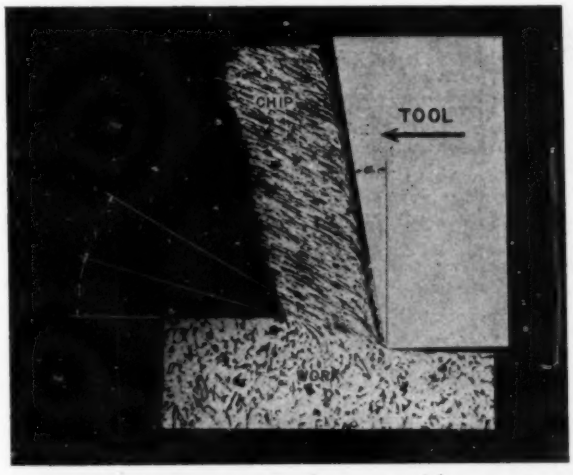

FIG. 2. Photomicrograph of chip obtained with negative rake sintered-carbide tool cutting SAE 1112 steel at 780 ft./min.
60×. $\alpha=-10°$, $\phi=16°$, $\psi=14°$.

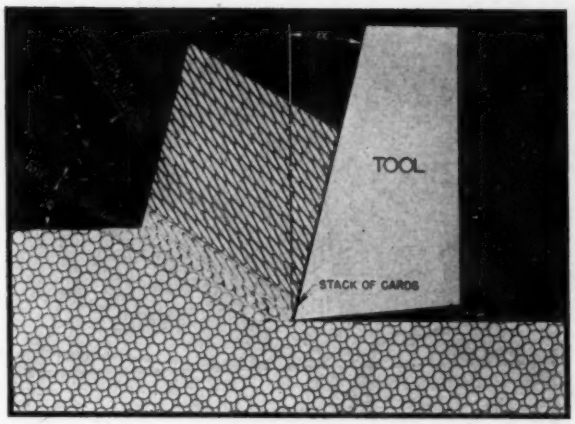

FIG. 3. Model, incorporating stack of cards, illustrating mechanism of formation of continuous chip and the resulting deformation of crystal structure.

angle. Thus the similarity between Figs. 2 and 3 is evident.

It is not difficult to derive the following expression from the geometry of Fig. 3:

$$\cot\psi=\cot\phi+\tan(\phi-\alpha), \qquad (1)$$

where ϕ is the shear angle, or angle which the plane of shear makes with the surface generated, and α is the true rake angle of the cutting tool, as designated in Fig. 3. The values of the three angles obtained by measurements on Fig. 2, as given in the caption to that figure, are found to satisfy Eq. (1).

It is fairly evident from the foregoing discussion that the angles ϕ and ψ must bear some relationship to the shearing strain undergone by the chip during the process of its formation. The physical significance of the shearing strain is illustrated in the schematic representation given in Fig 4. The card-like elements displaced by the cutting tool are assumed to have a finite thickness ΔX (though in the actual cutting of metal $\Delta X\rightarrow 0$). Then each element of thickness ΔX is displaced through a distance ΔS with respect to its neighbor, during the formation of the chip. Thus, if the shearing strain be denoted by ϵ, then

$$\epsilon=\Delta S/\Delta X,$$

and from the geometry of Fig. 4 it can then be found that

$$\epsilon=\cot\phi+\tan(\phi-\alpha). \qquad (2)$$

Comparing Eq. (2) with Eq. (1) it is evident that

$$\epsilon=\cot\psi. \qquad (2a)$$

Thus the angle ψ in photomicrographs such as

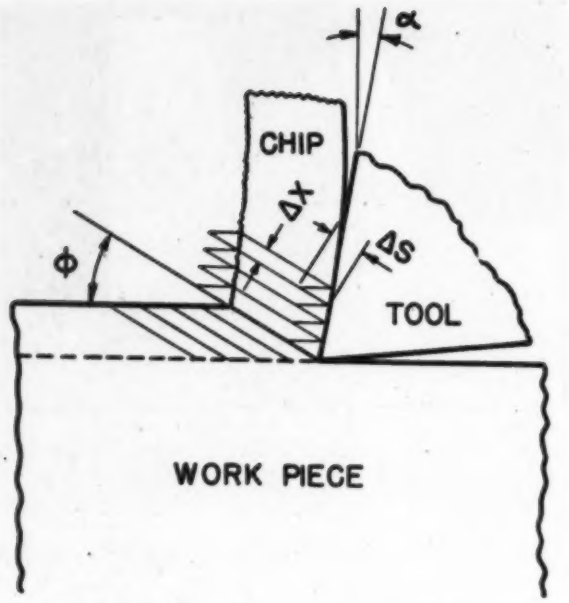

FIG. 4. Schematic representation of shearing strain, ϵ, in orthogonal cutting process. $\epsilon=\Delta S/\Delta X$. (In practice $\Delta X\rightarrow 0$.)

Fig. 2 takes on enhanced physical significance. The shearing strain given by Eqs. (2) or (2a) is the so-called "natural strain," since the product of it by the mean shear strength of the work material gives the work done in shear per unit volume of metal removed (see Eq. (15)).

The rate of shear is another geometrical quantity of interest. The relationship between the velocity of shear, V_s, the cutting velocity V_c, and the velocity of chip flow V_f, is shown in Fig. 5. This geometry is based on the fact that the velocity of the chip relative to the workpiece (V_s) must equal the vector sum of the velocity of the chip relative to the tool (V_f) and the velocity of the tool relative to the workpiece (V_c). The following expressions can be derived from the geometry of Fig. 5.

$$V_s=V_c\cos\alpha/\cos(\phi-\alpha), \tag{3}$$

$$V_f=V_c\sin\phi/\cos(\phi-\alpha). \tag{4}$$

B. Experiment

The application of Eqs. (1) through (4) to experiment requires that measurement be made of the angle ϕ. In practice, it is not usually convenient to make direct measurement of the shear angle, and therefore an accurate indirect method has been developed. From the schematic representation of the geometry of chip formation shown in Fig. 6 it can be seen that the ratio of the thickness, t_1, of the "chip" before removal to the mean thickness, t_2, of the chip after removal is a function of ϕ and α. This ratio, which is termed the "chip thickness ratio," r_t, is found from the geometry of Fig. 6 to be

$$r_t=t_1/t_2=\sin\phi/\cos(\phi-\alpha). \tag{5}$$

Therefore

$$\tan\phi=r_t\cos\alpha/1-r_t\sin\alpha. \tag{5a}$$

Equation (5a) is not very satisfactory for determining ϕ as it stands, since the mean thickness, t_2, of the chip after removal is usually difficult to measure because of the roughness of the exterior chip surface. However, in orthogonal cutting the chip is virtually the same width before and after removal, and therefore the ratio of the length, L_2, of the chip after removal to its length, L_1, before removal—called the chip length ratio, r_L—is equal to the chip thickness ratio.* Thus

$$r_L=L_2/L_1=t_1/t_2=r_t. \tag{6}$$

Equation (5a) then becomes

$$\tan\phi=r_L\cos\alpha/(1-r_L\sin\alpha). \tag{7}$$

Equation (7) can be used very readily to determine ϕ, since the chip length ratio is easily determined by any one of several different methods. One of the most precise and versatile of these, and the one now generally employed in this

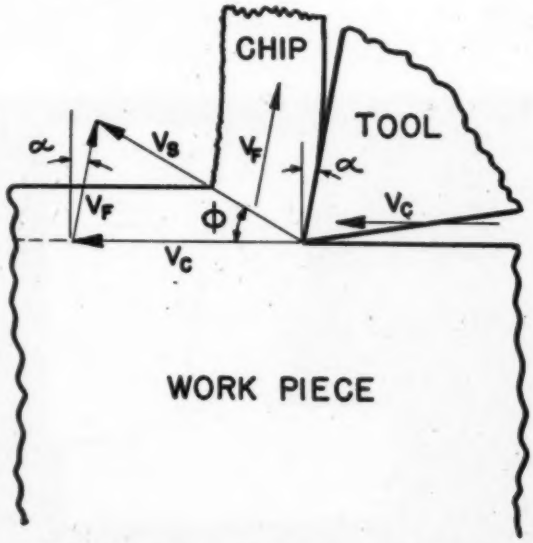

FIG. 5. Velocity relationships in orthogonal cutting.

* It should be noted here that the chip length ratio has been given the special name of "cutting ratio," designated by r_c, for reasons set forth in an earlier paper (see reference 1).

laboratory, is to weigh accurately a known length of the chip. The chip length ratio is then found by dividing the calculated weight of the same length of chip before removal by this observed weight, thus

$$r_L = t_1 w_1 \rho / m, \qquad (8)$$

where w_1 = width of chip, ρ = density of material being cut, and m = observed weight per unit length of chip.

In order to give an idea of the range of values of the geometrical quantities ϕ, ϵ, V_s/V_c, V_f/V_c, and r_L which may be encountered in experiment, values found in a typical cutting test are compiled in Table I. The material cut was N.E. 9445 steel of 187 Brinell hardness number, and the cutting tool was of the sintered-carbide type. The workpiece used was of tubular form, similar to that employed by Stanton and Hyde.[3] The tube was rotated about its central axis and the straight-edged cutting tool fed in a direction parallel to the axis, thus continually shortening the tube by removing a chip from its end surface. (See Fig. 10.) This satisfied the condition that the cutting be done by a *single* straight edge. In such an arrangement the chip width, w_1, is the wall thickness of the tube, while the thickness, t_1, of the "uncut chip" is equal to the feed of the tool per revolution of the tubular workpiece. The chip obtained in these tests was of type 2.

In connection with Table I, the high values found for ϵ perhaps require some explanation. Ordinarily, steel cannot be subjected to such high values of shearing strain at room temperature without undergoing rupture. The fact that chips obtained at such high values of shearing strain can be, and are, continuous may be attributed to two factors present in the cutting process. The first of these is the high compressive stress acting on the shear plane (see Table II). Bridgman[4] has demonstrated that the strain necessary to produce rupture in shear increases quite rapidly as the compressive stress on the plane of shear is increased. The second factor which helps prevent rupture, especially at high cutting speeds, is the heat generated at the shear plane by the shearing process. It is well known that the ductility or strain-hardening capacity of steel increases with increasing temperature.

It may be noted from Table I that the values of V_f/V_c and r_L are identical. A comparison of Eqs. (4) and (5) makes plain the reason for this.

TABLE I. Values of geometrical quantities in a typical test. Work material—NE 9445 steel; tool material—sintered carbide; width of cut (w_1)—0.25 in.

t_1 in./1000	Observed V_c (mean) ft./min.	α	r_L	Calculated ϕ	ϵ	V_s/V_c	V_f/V_c
3.70	197	+10°	0.29	17.0	3.4	0.99	0.29
	400		.33	19.0	3.1	1.00	.33
	642		.37	21.5	2.7	1.01	.37
	1186		.44	25.0	2.4	1.02	.44
3.70	400	−10°	.32	16.5	3.9	1.10	.32
	637		.37	19.0	3.5	1.13	.37
	1160		.44	22.0	3.1	1.16	.44
1.09	542	+10°	.33	19.0	3.1	1.00	.33
2.34			.32	18.5	3.1	1.00	.32
3.70			.37	21.5	2.7	1.01	.37
7.88			.44	25.0	2.4	1.02	.44
1.09	542	−10°	.23	12.5	5.0	1.07	.23
2.34			.30	16.0	4.0	1.10	.30
3.70			.37	19.0	3.5	1.13	.37
7.88			.46	22.5	3.1	1.17	.46

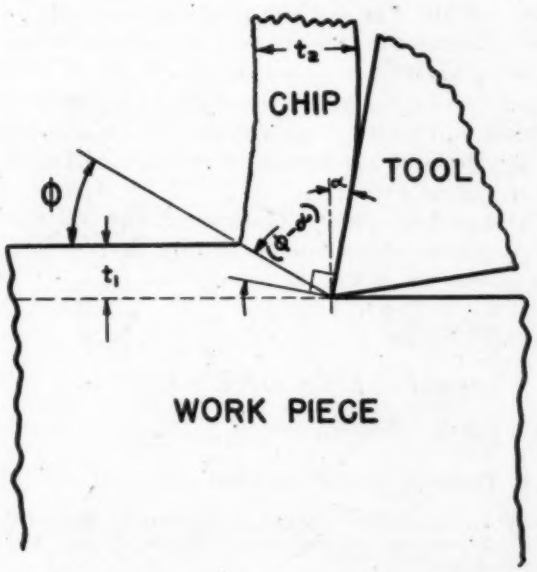

FIG. 6. Chip geometry in orthogonal cutting.

FORCE RELATIONSHIPS IN ORTHOGONAL CUTTING

A. Theory

A physically consistent picture of the nature of the force system associated with the cutting process is an essential to the analysis of the mechanics of the system. A simple approach to the obtaining of such a picture is to treat the

[3] T. E. Stanton and J. H. Hyde, Proc. Inst. Mech. Eng. 99, 175–194 (1925).

[4] P. W. Bridgman, J. App. Phys. 14, 273–283 (1943).

TABLE II. Values of forces and related quantities in a typical test. Work material—NE 9445 steel; tool material—sintered carbide; width of cut (w_1)—0.25 in.

Observed					Calculated							
t_1 in./1000	V_c (mean) ft./min.	α	F_c lbs.	F_t lbs.	μ	F lbs.	F_s lbs.	S_s psi.	S_n psi.	W_f/W_c	W_s/W_c	W_c in.-lb./in.^{3}
3.70	197	+10°	370	273	1.05	335	270	85,000	115,000	0.27	0.73	400,000
	400		360	283	1.11	345	250	88,000	137,000	.32	.68	390,000
	642		329	217	.95	270	230	90,000	129,000	.30	.70	355,000
	1186		303	168	.81	220	205	93,000	130,000	.32	.68	330,000
3.70	400	−10°	416	385	.64	310	290	89,000	153,000	.24	.76	450,000
	637		384	326	.58	255	255	90,000	152,000	.25	.75	415,000
	1160		356	263	.51	200	230	94,000	154,000	.25	.75	385,000
1.09	542	+10°	127	101	1.12	120	85	103,000	164,000	.33	.67	460,000
2.34			242	186	1.08	225	170	92,500	140,000	.30	.70	410,000
3.70			336	226	.96	280	230	91,000	131,000	.31	.69	360,000
7.88			605	315	.76	420	415	89,000	116,000	.31	.69	310,000
1.09	542	−10°	181	198	.78	165	130	103,000	179,000	.22	.78	670,000
2.34			295	291	.70	230	205	96,000	172,000	.23	.77	500,000
3.70			401	350	.60	275	265	94,000	164,000	.29	.71	430,000
7.88			698	472	.46	345	465	90,000	138,000	.23	.77	350,000

chip as a "separate" body in stable mechanical equilibrium under the action of two equal, opposite resultant forces**—the force which the tool exerts on the back surface of the chip and the force which the workpiece exerts on the base of the chip (shear plane). The resulting force system for the case of orthogonal cutting is shown in Fig. 7, in which R and R' represent the two equal, opposite forces which hold the chip in equilibrium. The force R' which the tool exerts on the chip may be resolved along the tool face into a component F, the friction force, which is responsible for the work expended in friction as the chip slides over the tool face and into a component N, the normal force, perpendicular to F. The angle τ between N and R' is the friction angle. The force R which the workpiece exerts on the chip may be resolved along the shear plane into a component F_s, the shearing force, which is responsible for the work expended in shearing the metal, and into a component F_n, which exerts a compressive stress on the shear plane and is perpendicular to F_s. Force R may also be resolved along the direction of motion of tool relative to work into a component F_c, the cutting force, which is responsible for the total work done in cutting, and into a component F_t, the thrust force, which is perpendicular to F_c.

** The fact that the two equal resultant forces are not exactly collinear is here neglected, since this fact plays no part in the present discussion. The effect of this lack of collinearity on the curl of the chip has been touched on briefly in replying to the discussion on an earlier paper (see reference 7).

Forces R and R' are equal and parallel and all their components may therefore be represented as components of a single vector R, located for convenience at the cutting edge. This has been done in Fig. 8, and the geometrical relationships existing between the various force components then become quite evident.

It appears that a force diagram similar to that shown in Fig. 7 was first developed by Piispanen,[5] in Finland, though the author was unaware of this when he[6] arrived at the force diagram given here, on the basis of the principles set forth in the foregoing discussion, and subsequently published it in collaboration with Ernst.[7] The Finnish paper was only recently brought to the author's attention. Piispanen apparently did not continue to develop the mechanics of orthogonal cutting to any great extent.

As has been shown elsewhere,[1] the following force relationships can be readily derived from the geometry of Fig. 8:

$$\mu = F/N = \tan \tau$$

$$= (F_t + F_c \tan \alpha)/(F_c - F_t \tan \alpha), \quad (9)$$

$$F = F_t \cos \alpha + F_c \sin \alpha, \quad (10)$$

[5] V. Piispanen, Teknillinen Aikakauslehti **27**, 315–322 (1937).

[6] M. E. Merchant, "Theory of Friction in Metal Cutting" (University of Cincinnati Thesis, D.Sc., 1940) (confidential).

[7] H. Ernst and M. E. Merchant, "Chip formation, friction and high quality machined surfaces," *Surface Treatment of Metals* (American Society for Metals, 1941), pp. 299–378.

$$F_s = F_c \cos \phi - F_t \sin \phi, \quad (11)$$

$$S_s = F_s/A_s = (F_c \sin \phi \cos \phi - F_t \sin^2 \phi)/A_0, \quad (12)$$

$$S_n = F_n/A_s = S_s \tan (\phi + \tau - \alpha), \quad (13)$$

$$W_f = Fr_c/A_0 = F/A_c, \quad (14)$$

$$W_s = S_s \epsilon, \quad (15)$$

$$W_c = S_s \epsilon + F/A_c = W_s + W_f. \quad (16)$$

In the above, μ = coefficient of friction between sliding chip and tool face, S_s = mean shear stress on shear plane = mean shear strength of material being cut, A_s = area of shear plane = $A_0/\sin \phi$, A_0 = cross-sectional area of "chip" before removal = $t_1 w_1$ (see Fig. 8), S_n = mean compressive or normal stress on shear plane, W_f = work expended in friction between chip and tool, per unit volume of metal removed, r_c = cutting ratio = r_L, A_c = cross-sectional area of chip after removal = A_0/r_c (see Fig. 8), W_s = work expended in shearing the metal, per unit volume of metal removed, and W_c = total work expended in cutting, per unit volume of metal removed. Other symbols are as previously defined.

Equation (16), derived from the geometry of Fig. 8, is of particular interest because it states that the total work expended in cutting is the sum of the work expended in friction between chip and tool and the work expended in shearing the metal. This logical result serves in the nature of a check on the correctness of the simple picture of the cutting process and its force system presented here.***

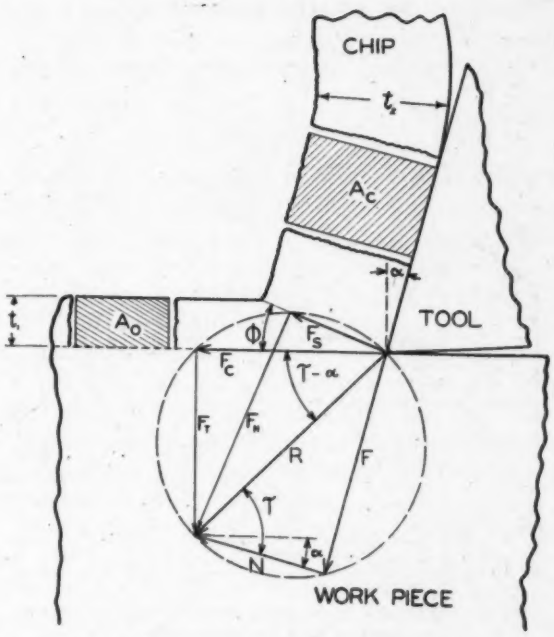

FIG. 8. Condensed force diagram showing relationships between components.

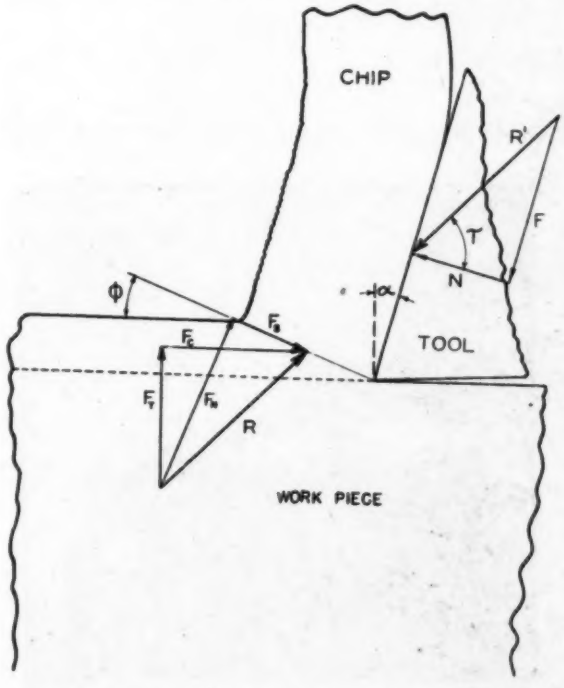

FIG. 7. Force system holds chip in stable mechanical equilibrium.

*** In the above analysis the work (and the accompanying force) required *to separate* the chip from the metal at the very cutting edge (thus producing two new surfaces) has not been considered because it is negligible in comparison with the total work expended in friction and in shear under all ordinary circumstances. This statement can be verified in part by a rough estimate, from the surface tension (surface energy) of the solid, of the work required to create the new surfaces on the chip and the workpiece. It is known that the surface energy of solid metals is very roughly of the order of 1000 ergs per sq. cm or about 0.006 in. lb. per sq. in. The amount of new surface produced in removing one cubic inch of metal by taking a chip having an original thickness, t_1, of, let us say, 0.001 inch is less than 2000 sq. inches ("less than," because the new surface produced on the work is 1000 sq. inches, whereas the new surface produced on the chip is equal to this figure multiplied by the chip length ratio, r_L). Therefore the amount of work, per unit volume of metal removed, required to create the new surfaces under these conditions is of the order of $2000 \times 0.006 = 12$ in. lb. per cu. in. Since the total work expended in cutting is of the order of 500,000 in. lb. per cu. in. in the case of steel, for example (see Table II), it is evident that the work required to create the surfaces is negligible in comparison. Only when the dimension t_1 became of the order of 0.00001" or less would the surface energy begin to become significant. It is virtually impossible to cut such a thin chip from metal.

The above estimate of the energy required to separate the chip from the metal at the very cutting edge would of course be increased somewhat by considering the work expended in the local plastic flow of the metal adjacent

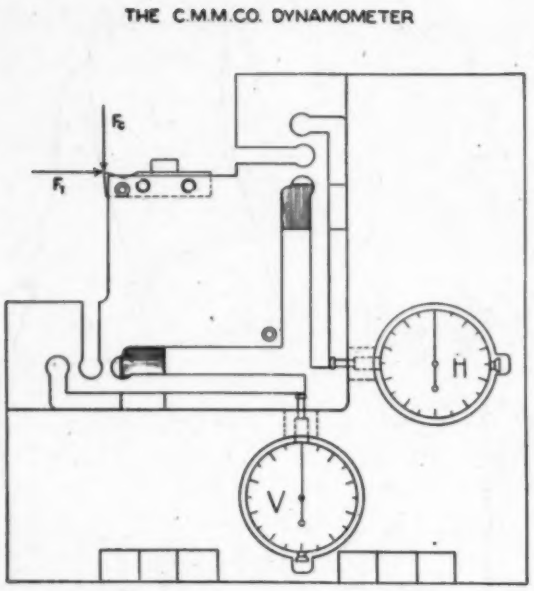

FIG. 9. Schematic view of internal structure of mechanical tool dynamometer.

B. Experiment

The quantities which must be observed in order to make an analysis of the force relationships presented above are t_1, w_1, V_c, α, ϕ, F_c, and F_t. The experimental methods used in connection with the observation of the purely geometrical quantities among these have already been discussed. The two force components F_c and F_t may be observed with any suitable tool dynamometer capable of measuring two mutually perpendicular components. In the case of orthogonal cutting with a tool having a single straight cutting edge there is no third force component, the force system being two-dimensional, as is evident from the preceding discussion of theory.

Many suitable tool dynamometers have been described in the literature as, for instance, an hydraulic unit described by Stanton and Hyde[3] and a recent electrical tool dynamometer described by Hand.[3]

to the newly created surfaces on chip and work. It is by virtue of this plastic flow that these surfaces come into being (no tensile failure occurs ahead of the cutting edge in the case of a type 2 chip.) However, this energy is also quite a small percentage of the total work, judging from the relatively small amount of local surface deformation revealed by photomicrographs such as Figs. 1 and 2. Therefore the energies and forces involved in creating the new surfaces on chip and work, being negligible in magnitude, are not considered in the analysis given in this paper.

[3] A. R. Hand, Gen. Elec. Rev. **44**, 605–607 (1941).

In the tests to be discussed here and in some later papers of this series, a simple mechanical tool dynamometer developed in this laboratory was used. A schematic view of the internal structure is shown in Fig. 9. An integral lever system actuates the dial-indicators as shown, to provide force readings. In Fig. 10 the dynamometer is shown in action cutting one of the tubular-type workpieces employed.

It is often the case with tool dynamometers that, despite careful precautions in the construction, the meter which is supposed to respond only to force F_c is affected slightly by force F_t, and *vice versa*. In this case special methods are necessary in order to obtain the forces from the meter readings. If for example the calibration is linear, as is often the case, the situation can be handled as follows. The process of calibration performed by applying first values of F_c alone, then of F_t alone, will yield four equations of the form

$$x=aF_c, \quad y=bF_c,$$
$$x=cF_t, \quad y=dF_t,$$

where x=any reading of one meter of the dynamometer, y=any reading of second meter of the dynamometer, and a, b, c, d=proportionality constants of the dynamometer. Then, when the dynamometer is in operation, any reading x is a function of both F_c and F_t, thus

$$x=aF_c+cF_t.$$

Likewise, for y

$$y=bF_c+dF_t.$$

Solving these two simultaneous equations for F_c

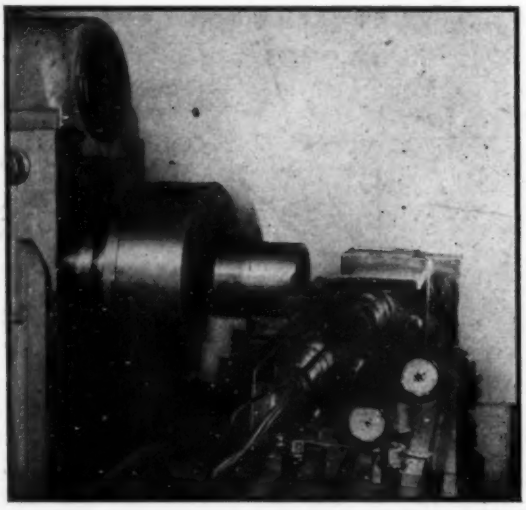

FIG. 10. Tool dynamometer in action.

and F_t yields

$$F_c=(dx-cy)/(ad-cb),$$
$$F_t=(ay-bx)/(ad-cb).$$

These are the equations used to compute the forces from the meter readings. They are readily handled by means of alignment charts. It is evident that similar though more complicated equations could be obtained in like manner if the meter readings are some function other than linear of the forces, provided this function can be obtained in analytic form from the calibration curves.

In order to give an idea of the range of values of μ, F, F_s, S_s, S_n, W_f, W_s, and W_c which may be encountered in experiment, values found in the same cutting tests which supplied the data for Table I have been compiled in Table II.

The high values found for μ may seem surprising. However, these are to be expected in the light of information presented by Ernst and Merchant.[7] The chip surface which rubs over the tool face is one which is freshly formed, or "nascent," and therefore free of all adsorbed films which would tend to reduce friction. The tool face is likewise wiped free of adsorbed films by this nascent surface. The friction involved is truly that of metal-on-metal, with no interposed adsorbed films of low shear strength, and is therefore high.

SUMMARY

Theory and equations have been presented by which it is possible, with little approximation, to analyze fairly extensively any orthogonal cutting process in which a continuous chip is produced in terms of basic quantities common to all of mechanics. The application of this theory to experiment yields reasonable results.

This analysis is a small but necessary step toward a general understanding of the mechanics of cutting, and provides a useful insight into the nature of the cutting process, as well as data of considerable practical value.

The author wishes to express his appreciation for the helpful comments and suggestions contributed by Mr. Hans. Ernst, Research Director, and for the able assistance of Mr. Norman Zlatin of this department who carried out most of the experimental work and calculations, and of Mr. Clarence Irwin, also of this department, who made the careful measurements of chip length ratio.

Optimum Height of Flight of Winged Rocket- or Jet-Bomb

M. Zbigniew L. Krzywoblocki
Brown University

(Received October 9, 1944)

The purpose of this note is to present the formulae for calculation of optimum height of horizontal flight of winged rocket- or jet-bomb in an elementary way. First, the elementary principles of rocket-propulsion are given, i.e., the momentary coefficient of external efficiency, which represents the part of the total energy of the propulsive material imparted to the rocket, the mass of the rocket after a certain time, the actual acceleration and the average acceleration of the rocket, and the average coefficient of external efficiency over a certain period of time. Next, the horizontal flight of a rocket in atmosphere at a certain height is considered and the formulae for the optimum height of flight are derived in two cases: (*a*) constant velocity of flight, (*b*) constant mass of the outflowing gases. The calculations refer to the case of adiabatic flow in the nozzle but may be applied easily to the case of any polytropic flow. The considerations are repeated in the same order for jet-propulsion. The formulae are derived under the simplifying assumption that the difference in pressures in the wake behind the bomb in flight—in which the pressure is smaller than in the free air—and in the free air may be disregarded, since it is assumed that at the mouth of the nozzle the pressure equals the pressure in the free air. The difference between rocket- and jet-propulsion is presumed to be known. In the former type of propulsion the propulsive material contains in itself the oxygen necessary for the combustion process, while in the latter the oxygen is taken from the outside air. The type of propulsion in which oxygen is contained, separately from the fuel, within the rocket in a compressed or liquid state, should be included in the rocket group.

1. FLIGHT WITHOUT TAKING THE AIR FROM OUTSIDE

ASSUME a purely theoretical case of flight of a winged rocket in a vacuum or in atmosphere with no resistance and no potential field. The exhaust gases flow out from the nozzle directly into the external space. Consequently:

$$F=m_s\cdot c, \qquad (1)$$

where F=reactional force of the outflowing gases, m_s=mass of the outflowing gases in 1 sec.,

and c = velocity of the outflowing gases with respect to the walls of the nozzle.

Assume the coefficient of the internal efficiency equal to unity. The total energy of a unit of mass of the propulsion material in the combustion chamber is equal:

$$L_1 = v^2/2 + c^2/2, \tag{2}$$

where v = momentary velocity of the rocket. The energy of a unit of mass of the gases (exit energy per unit mass of the gases):

$$L_2 = (c-v)^2/2. \tag{3}$$

The increase in energy of the rocket:

$$L = L_1 - L_2 = vc. \tag{4}$$

The momentary coefficient of the external efficiency of the rocket:

$$\eta = L/L_1 = 2vc/(c^2+v^2). \tag{5}$$

This coefficient reaches the maximum value for c = constant and v variable:

$$d\eta/dv = 0, \tag{6}$$

$$\eta_{max} = 1, \tag{7}$$

for

$$v = c. \tag{8}$$

If dm denotes the mass of the outflowing gases in the time dt, m the remained mass of the rocket and dv the increase in velocity of the rocket, then:

$$c \cdot dm = -m \cdot dv, \tag{9}$$

or

$$c \cdot dm/dt = -m \cdot dv/dt. \tag{10}$$

Assumption that

$$dv/dt = a = \text{const.}, \tag{11}$$

and integration between limits $t=0$ and $t=t_1$ lead to:

$$c \cdot \int_{m_0}^{m_1} dm/m = -a \int_0^{t_1} dt, \tag{12}$$

$$m_1 = m_0 \cdot e^{-at_1/c}. \tag{13}$$

Equation (13) gives the mass of the rocket flying with a constant acceleration a after the time t_1 (Hohmann).

Assumption that the mass of the outflowing gases in the time dt is constant:

$$dm/dt = k = \text{const.}, \tag{14}$$

gives

$$c \cdot k = -m \cdot p_t, \tag{15}$$

where p_t = variable actual acceleration after the time t. Since:

$$m = m_0 - \int_0^t (dm/dt) \cdot dt = m_0 - k \cdot t. \tag{16}$$

Consequently the average acceleration is:

$$p_{ta} = -c \cdot k/(m_0 - k \cdot t). \tag{17}$$

The sign minus means that the directions of p_{ta} and c are opposite. The value of p_{ta} may be given by a different formula. From Eq. (9):

$$-c \int_{m_0}^{m_1} dm/m = \int_{v_0}^{v_1} dv, \tag{18}$$

or

$$c \cdot \ln (m_0/m_1) = v_1 - v_0. \tag{19}$$

The limitation of time to 1 sec. gives the value of the acceleration after the first second:

$$p_{1a} = c \cdot \ln (m_0/m_1) = c \cdot \ln [m_0/(m_0-k)]. \tag{20}$$

After t seconds:

$$p_{ta} = c \cdot \ln [(m_0-(t-1)\cdot k)/(m_0 - t \cdot k)]. \tag{21}$$

Assume at the beginning of the flight the mass m_0 and the velocity v_0, after time t_1, m_1, and v_1. Only the first and the last moments of the flight are taken into account. The increase in energy of the mass m_1:

$$\Delta L_i = m_1 \cdot (v_1^2 - v_0^2)/2. \tag{22}$$

The loss of energy in form of the exhaust gases:

$$\Delta L_g = (m_0 - m_1) \cdot c^2/2. \tag{23}$$

The lost energy of the rocket:

$$\Delta L_r = (m_0 - m_1) \cdot v_0^2/2. \tag{24}$$

The average coefficient of the external efficiency in the period t_1:

$$\eta_a = \frac{\Delta L_i}{\Delta L_g + \Delta L_r} = \frac{v_1^2 - v_0^2}{(m_0/m_1 - 1)\cdot(v_0^2 + c^2)}. \tag{25}$$

Application of Eq. (19) gives:

$$\eta_a = (v_1^2 - v_0^2)/[(e^{(v_1-v_0)/c} - 1)\cdot(v_0^2 + c^2)]. \tag{26}$$

For

$$v_0 = 0, \tag{27}$$

$$\eta_a = (v_1/c)^2/(e^{v_1/c} - 1), \tag{28}$$

which is in accordance with formula given by

Sänger and Oberth. In the last case from:

$$d\eta_a/d(v_1/c)=0, \tag{29}$$

$$\eta_{a\,\max}=0.617, \tag{30}$$

for

$$v_1/c=1.593. \tag{31}$$

In the next step consider atmospheric resistance and potential field (gravitation). Assume a winged rocket flying horizontally in atmosphere at a certain height h. At any moment the reactional force of the outflowing gases is equal to the drag of the rocket:

$$c_D\cdot(A/2)\cdot\rho_2\cdot v^2=m_s\cdot c_2+S(p_2-\bar{p}_2), \tag{32}$$

where c_D = drag coefficient of the rocket, A = wing area of the rocket, ρ_2 = density of the air at the height h, c_2 = velocity of gases at mouth of the nozzle, S = nozzle area at mouth, p_2 = pressure of the propulsion gas at mouth of nozzle, and $\bar{p}_2$ = pressure of outside air at the height h. Assumption, that the construction and the length of the nozzle permit to reach $p_2=\bar{p}_2$ gives:

$$c_D\cdot(A/2)\cdot\rho_2\cdot v^2=m_s\cdot c_2. \tag{33}$$

Case a.

Assume v = const., consequently a change in weight and lift of the rocket during the flight causes changes in value of c_D and m_s but so that

$$m_s:c_D=\text{const.} \tag{34}$$

In other words a change in angle of attack causes a change of the mass of the outflowing gases. Strictly speaking, in order to maintain a constant velocity c_2, the change of angle of attack should cause also a change in dimensions of the nozzle which leads to a purely theoretical case. In accordance with the International Standard Atmosphere:

$$\rho_2=p_2^{1/1.235}\rho_0/(p_0^{1/1.235}), \tag{35}$$

where ρ_0, p_0 refer to the sea-level. Assumption of an adiabatic flow in the nozzle leads to:

$$c_2=\{[2gn/(n-1)]\cdot p_1\cdot V_1\cdot[1-(p_2/p_1)^{(n-1)/n}]\}^{\frac{1}{2}}, \tag{36}$$

where n = ratio of specific heats at constant pressure and constant volume, p_1 = pressure in the combustion chamber, and V_1 = specific volume of the propulsion gas in the combustion chamber.

Equation (36) is derived under the assumption that the velocity of the gas in the combustion chamber equals zero. Substitution of Eqs. (35) and (36) into Eq. (33) leads to:

$$v=(b\cdot d)^{\frac{1}{2}}[1-(p_2/p_1)^{(n-1)/n}]^{\frac{1}{2}}/p_2^{1/2.47}, \tag{37}$$

$$b=2\cdot m_s/[c_D\cdot A\cdot(\rho_0/p_0^{1/1.235})], \tag{38}$$

$$d=\left(\frac{2gn}{n-1}\cdot p_1\cdot V_1\right)^{\frac{1}{2}}. \tag{39}$$

The maximum external efficiency will be reached for $v=c_2$, Eq. (8), or for:

$$b=d\cdot p_2^{1/1.235}[1-(p_2/p_1)^{(n-1)/n}]^{\frac{1}{2}}. \tag{40}$$

Assume that the pressure and temperature inside the combustion chamber do not depend on the altitude and that they are constant for the given propulsion material. Equation (40) gives the relationship between p_1 and p_2. The relationship between p_2 and h may be found from the formula of the International Standard Atmosphere:

$$p_2/p_0=[1-0.00000688h]^{5.256}. \tag{41}$$

For stratospheric flights more precise formulae may be used.

Case b.

Assume m_s = const. and v variable but so that the product $c_D\cdot v^2$ is a constant value. In other words the velocity varies as $1/(c_D)^{\frac{1}{2}}$. From Eq. (33) and from the equation for lift:

$$W=c_L\cdot(A/2)\cdot\rho_2\cdot v^2, \tag{42}$$

where W = variable weight of the bomb, one obtains:

$$W=m_s\cdot c_2\cdot c_L/c_D=\text{const.}\cdot c_L/c_D. \tag{43}$$

Since the weight of the bomb W decreases in the course of flight, the ratio c_L/c_D and consequently the angle of attack must also decrease. The relationship between the ratio c_L/c_D and the angle of attack may be given by the polar diagram of the bomb.

Let v_1 be the velocity in the moment, the total propulsion material is burnt and the bomb starts to glide. Assumption that the motion begins with the initial velocity equal to zero, leads to the conclusion that the value of the velocity v_1 should be equal to

$$v_1=1.593c_2. \tag{44}$$

The value of v_1 is given by Eq. (37) in which c_D corresponds to angle of attack in the moment the last part of the propulsion material is burning. Substitution of Eqs. (36) and (37) into Eq. (44) leads to:

$$b=1.593^2\cdot d\cdot p_2^{1/1.235}\cdot[1-(p_2/p_1)^{(n-1)/n}]^{\frac{1}{2}}. \quad (45)$$

Equation (45) permits one to find the optimum value of p_2.

In the case when the initial velocity v_0 is not equal to zero, Eq. (26) may be represented in the form

$$\eta_a=\frac{v_1^2/c^2-v_0^2/c^2}{(e^{v_1/c-v_0/c}-1)(v_0^2/c^2+1)}. \quad (46)$$

Assuming $v_0/c=$const. one can easily find from Eq. (29) the optimum value of v_1/c and the value of $\eta_{a\,max}$. The subsequent procedure remains the same.

2. FLIGHT WITH TAKING THE AIR FROM OUTSIDE

The above derived equations are valid for rocket propulsion (oxygen is contained in the propulsive material itself) or for jet-propulsion without taking the air from outside (oxygen is contained in the bomb itself in liquid form). When the air is taken from outside, the formulae are different. The simplest possible type of construction of a winged jet-bomb will be considered, i.e., a nozzle with a valve in the front part and with a fuel injection device. The air enters in the front with the velocity v and leaves with the velocity c by virtue of the combustion of the fuel. The corresponding formulae for the case of flight in atmosphere with no resistance and no potential field:

$$F=\alpha\cdot m_f\cdot(c-v)+m_f\cdot c, \quad (1')$$

where $\alpha\cdot m_f=$mass of the air, $\alpha=$air fuel ratio by weight, and $m_f=$mass of the fuel.

$$L_1=\alpha\cdot m_f\cdot c^2/2+m_f\cdot(v^2+c^2)/2, \quad (2')$$

$$L_2=(\alpha+1)\cdot m_f\cdot(c-v)^2/2, \quad (3')$$

$$L_3=\alpha\cdot m_f\cdot v^2/2. \quad (3'')$$

$$L=L_1-L_2-L_3$$

$$=[(\alpha+1)\cdot m_f\cdot c-\alpha\cdot m_f\cdot v]\cdot v. \quad (4')$$

Since

$$(\alpha+1)=\sim\alpha \text{ (approx.)}, \quad (4'')$$

$$L=(\alpha+1)\cdot m_f\cdot(c-v)\cdot v \text{ (approx.)}, \quad (4''')$$

$$\eta=\frac{L}{L_1}=\frac{2[(\alpha+1)\cdot c-\alpha\cdot v]\cdot v}{(\alpha+1)\cdot c^2+v^2}. \quad (5')$$

Neglecting $m_f\cdot v^2/2$ in Eq. (2') and application of Eq. (4'') lead to:

$$\eta=2(c-v)\cdot v/c^2. \quad (5'')$$

For $c=$constant and $\alpha=$constant:

$$d\eta/dv=0, \quad (6')$$

$$\eta_{max}=\alpha+1/[\alpha+(\alpha^2+\alpha+1)^{\frac{1}{2}}], \quad (7')$$

for

$$c=[\alpha v+v(\alpha^2+\alpha+1)^{\frac{1}{2}}]/(\alpha+1). \quad (8')$$

Application of Eq. (5'') gives:

$$\eta_{max}=\tfrac{1}{2}, \quad (7'')$$

for

$$c=2\cdot v. \quad (8'')$$

Similarly other equations can be changed:

$$c\cdot d[(\alpha+1)\cdot m_f]-v\cdot d(\alpha\cdot m_f)=-m\cdot dv. \quad (9')$$

$$-\int_{m_0}^{m_1}\frac{dm_f}{m}=-\frac{1}{\alpha}\int_{v_0}^{v_1}\frac{\alpha\cdot dv}{v\cdot\alpha-c(\alpha+1)}. \quad (18')$$

$$\ln\frac{m_0}{m_1}=\frac{1}{\alpha}\left[\ln\frac{v_0\cdot\alpha-c(\alpha+1)}{v_1\cdot\alpha-c(\alpha+1)}\right]. \quad (19')$$

Eqs. (22), (23), and (24) will remain unchanged. Besides that the energy of the air must be taken into account:

$$\Delta L_a=\alpha\cdot(m_0-m_1)\cdot c^2/2. \quad (24')$$

$$\eta_a=\frac{\Delta L_i}{\Delta L_g+\Delta L_r+\Delta L_a}$$

$$=\frac{v_1^2-v_0^2}{(m_0/m_1-1)[c^2(\alpha+1)+v_0^2]}. \quad (25')$$

$$\eta_a=\frac{v_1^2-v_0^2}{\left\{\left[\frac{v_0\cdot\alpha-c(\alpha-1)}{v_1\cdot\alpha-c(\alpha+1)}\right]^{1/\alpha}-1\right\}\cdot[c^2(\alpha+1)+v_0^2]}. \quad (26')$$

For $v_0=0$

$$\eta_a=\frac{v_1^2/c^2}{\left\{\left[\frac{-(\alpha+1)}{(v_1/c)\cdot\alpha-(\alpha+1)}\right]^{1/\alpha}-1\right\}(\alpha+1)}. \quad (28')$$

Case a.

$$c_2=\left\{\frac{2\cdot g\cdot n}{n-1}\cdot p_1\cdot V_1\cdot\left[1-\left(\frac{p_2}{p_1}\right)^{(n-1)/n}\right]+v^2\right\}^{\frac{1}{2}}. \quad (36')$$

This equation takes into account the entering velocity of the air v in the combustion chamber. Application of Eqs. (33), (8″) and (36′) leads to:

$$2b=(1/3)^{\frac{1}{2}}\cdot d\cdot p_2^{1/1.225}[1-(p_2/p_1)^{(n-1)/n}]^{\frac{1}{2}}. \quad (40')$$

Case b.

Equation (26′) permits one to find the optimum value of v_1/c for the given values of α and v_0/c, when η_a reaches its maximum value $\eta_{a\,\max}$. Substitution of obtained results into Eq. (33) together with Eq. (36′) solves the problem. The procedure is quite similar to that given above.

In all consideration given above the influence of the difference in pressures in the wake behind the bomb in flight—in which the pressure is smaller than in the free air—and in the free air was disregarded for the sake of simplicity, i.e., the assumption was made that at the mouth of the nozzle the pressure equals the pressure in the free air.

Deflection Sensitivity of Parallel-Wire Lines in Cathode-Ray Oscillographs*

H. Gunther Rudenberg†
Cruft Laboratory and Research Laboratory of Physics, Harvard University, Cambridge, Massachusetts

(Received November 10, 1944)

The deflection angle θ of a cathode-ray beam accelerated by a potential V is shown to be proportional to the linear charge density ρ transverse to the beam on the interior of the electrostatic deflection system, $\theta=\rho/2V\epsilon_0$. The voltage deflection sensitivity depends on the plate-to-plate capacitance c per unit width, $\theta/E=c/2V\epsilon_0$. This includes edge effects and permits a determination of the sensitivity from capacitance measurements or a simple graphical evaluation from the dimensions of the deflection system. The use of parallel-wire lines as a deflection system is suggested, and its deflection sensitivity evaluated. Such lines have low transit time error and are either easily tuned, or can be operated non-resonant with resistive termination.

1. INTRODUCTION: THE OUTPUT AMPLIFIER STAGE

THE major limitation upon the high frequency characteristics of a wide-band oscillograph is found to be in the output amplifier stage, which has to supply the shunting output capacitance of the tube and circuit. Considerable information on the design and frequency compensation of such amplifiers and their coupling networks is available in the literature[1–3] and will not be considered here. In order to determine the high frequency output voltage available for the oscillograph deflection system, an equation for the output of an uncompensated amplifier will be reviewed briefly. This will also give some information regarding the output of a similar compensated amplifier.

It will be assumed that, as is usually the case in practice, the output stage operates as a Class A amplifier. The peak output voltage E obtainable at the angular frequency ω is thus

$$E=I_pR/(1+j\omega CR). \quad (1a)$$

This reduces to

$$E=I_pR \quad (1b)$$

at low frequencies (Fig. 1). Here I_p is the peak output current available from the tube at very high frequencies without distortion, C the total tube, circuit, and oscillograph shunt capacitance, and R the equivalent a.c. resistance of the tube and the circuit considered in parallel.[4]

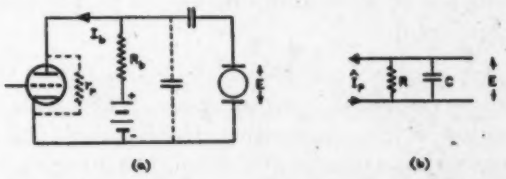

FIG. 1. (a) High frequency amplifier. (b) Equivalent circuit.

* Paper presented at the meeting of the New England Section of the American Physical Society at Brown University, Providence, Rhode Island, on October 28, 1944.

† Now U. S. Army, Corps of Engineers.

[1] F. E. Terman, *Radio Engineers' Handbook* (McGraw-Hill Book Company, Inc., New York, 1943), p. 434.

[2] H. A. Wheeler, Proc. I.R.E. 27, 429 (1939).

[3] D. E. Foster and J. A. Rankin, RCA Rev. 5, 409 (1941).

[4] E. L. Chaffee, *Theory of Thermionic Vacuum Tubes* (McGraw-Hill Book Company, Inc., New York, 1933), p. 199; reference (1), p. 357.

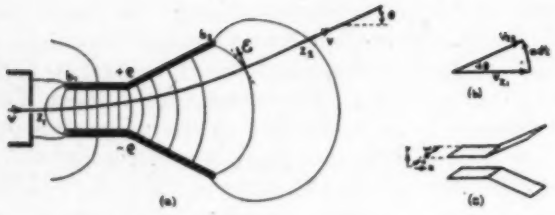

FIG. 2. (a) Cross section of cathode-ray tube deflection system. (b) Velocity vector diagram.

The frequency at which, with unchanged input voltage, the magnitude of the output voltage of the uncompensated amplifier stage is reduced to $1/\sqrt{2}$ of its low frequency value is sometimes called the upper limiting frequency of this stage. At this angular frequency ω' the shunt reactance of the output capacitance is equal to the equivalent resistance,

$$R=1/\omega' C. \tag{2}$$

Among other considerations, the equivalent resistance R is determined by the tube characteristics and the output voltage and frequency response required, while C is generally determined by the circuit and tube configurations. It is then convenient to determine the relation between these quantities and the limiting angular frequency ω' by substituting (2) into Eq. (1b). Thus the low frequency output voltage obtained under these conditions from the amplifier can be written

$$E=I_p/\omega' C. \tag{3a}$$

Under the assumption that the Class A amplifier of Fig. 1(a) is an ideal distortionless amplifier operated under conditions giving a maximum output current, the theoretical maximum of this peak alternating current I_p will be almost equal to the average current $\bar{I}_b$ drawn by the tube. With $\bar{I}_b=I_p$ we obtain, analogous to Terman,[1] a "figure of merit"

$$\bar{I}_b/C=E\omega' \tag{3b}$$

for the amplifier output stage. This gives the relation of the quantities which should be determined by compromise when designing such an amplifier. By using inductance or filter high frequency compensation[2,3] which provides a reactive energy storage to supply the reactive charging currents drawn by the shunt output capacitance, the high frequency response of the amplifier may be improved considerably.

In order to obtain a favorable high frequency response, the capacitance C should be reduced as much as possible. This can be achieved by a careful choice of tubes and proper circuit design. Secondly, the available a.c. tube current may be increased by using a tube and operating conditions where a larger average tube current is drawn. But the use of tube capable of handling higher currents entails relatively large power expenditures. An improvement in the high frequency response of an output amplifier stage can also be obtained by the use of negative feedback to reduce distortion. This would allow larger a.c. currents to be obtained for the same average tube current without exceeding any distortion limits.

Another possibility lies in the reduction of the voltage E necessary to deflect the oscillograph electron beam by increasing the sensitivity of its deflection system. An increased sensitivity, even with an increased deflection-plate capacitance, may provide a better compromise between the amplifier output-circuit capacitance and the oscillograph deflection system. Or else, when operating at fixed frequencies, the amplifier circuit and the deflection system can be tuned to these frequencies in order to supply the capacitive charging currents to the system without a large supply and expenditure of power in the amplifier. These last two possibilities will be considered in this paper.

2. VOLTAGE AND CHARGE SENSITIVITY OF AN ELECTROSTATIC DEFLECTION SYSTEM FOR SMALL TRANSIT TIMES

Referring to Fig. 2(a), the longitudinal velocity v of the electrons in the beam should remain substantially constant during their passage through the deflection system shown, in order to prevent defocusing of the beam at large deflections. As the vertical or y deflection has to be independent of the horizontal or x position of the beam between the plates, the field strength between the plates should be independent of x, and will therefore be considered uniform across the central part of the width w of the plates. The component ε of the electric field strength which is perpendicular to the beam path will act on each electron of mass m and charge e to produce an acceleration a which is also perpendicular to this path. Therefore, by Newton's law,

$$ma=e\varepsilon. \tag{4}$$

The change of angle θ of the beam produced while traveling through the deflection field is obtained from a consideration of the acceleration a acting perpendicular to the electron velocity v [Fig. 2(b)]. This gives

$$d\theta/dt=a/v=(e\varepsilon/mv). \tag{5a}$$

Integrating over the time interval t_1t_2 which the electron spends within the deflection field, we obtain

$$\theta=\frac{e}{m}\int_{t_1}^{t_2}\frac{\varepsilon}{v}dt, \tag{5b}$$

and substituting $dt=dz/v$

$$\theta=\frac{e}{m}\int_{z_1}^{z_2}\frac{\varepsilon}{v^2}dz. \tag{6}$$

Here z_1 is the position of the beginning and z_2 that of the end of the deflection field. The electrons in the beam have been accelerated to the velocity v previous to entering the deflection system by an acceleration potential V which is the mean d.c. potential of the two deflection plates with respect to the cathode of the electron gun. Usually V is the same as the second anode potential. Therefore $eV=\frac{1}{2}mv^2$ and thus

$$\theta=\int_{z_1}^{z_2}\frac{\varepsilon}{2V}dz. \tag{7a}$$

Under the assumption made above that v, and thus V, is constant while the electrons pass from z_1 to z_2 through the deflection field, we can place V before the integral and write

$$\theta=\frac{1}{2V}\int_{z_1}^{z_2}\varepsilon dz. \tag{7b}$$

To a better approximation, V is an average value of the potentials traversed by the beam during its passage through the deflection system.

The first and last lines of force which the beam crosses at z_1 and z_2 end at b_1 and b_2 on the upper deflection plate. We shall apply Gauss's theorem in two dimensions to the area enclosed by the electron path from z_1 to z_2, a line inside one deflection plate from b_1 to b_2, and the first and last lines of force z_1b_1 and z_2b_2. Gauss's theorem states that the charge enclosed within such an area is proportional to the integral of the perpendicular component of the field strength taken around the circumference. There is no component of the field strength perpendicular to the field lines z_1b_1 and z_2b_2, and the field is zero inside the metal deflection plates from b_1 to b_2. Thus, if ρ is the charge per unit width w of the plates within the limits b_1 and b_2 [Fig. 2(a)], we obtain

$$\int_{z_1}^{z_2}\varepsilon dz=\rho/\epsilon_0 \tag{8}$$

and therefore

$$\theta=\rho/2V\epsilon_0. \tag{9}$$

ρ is that portion of the linear charge density on the deflection plates which is between b_1 and b_2 and which is active in producing the deflection; ϵ_0 is the permittivity or dielectric constant of free space, $1/(36\pi\times10^9)$ farad per meter in m.k.s. units. If E is the voltage between the deflection plates, and c is the capacitance per unit width w of the deflection plates, related to that portion of the electrostatic field of the plates which the beam traverses, then

$$\rho=cE,$$

and thus

$$\theta=Ec/2V\epsilon_0. \tag{10}$$

The factor c is the plate-to-plate capacitance of the deflection system divided by its width w, the field strength being uniform over w. For a deflection system with lateral edge effects the factor c refers to the central cross section of the system. It does not include any capacitance of either deflection plate to the electron gun, to the leads, to other electrodes, or to ground. These are best considered as the external stray capacitances. The capacitance per unit width determines the voltage deflection sensitivity θ/E of any arbitrarily shaped deflection system, and can easily be obtained from simple capacitance measurements. The only precaution to be observed in such measurements is that the true plate-to-plate capacitance must be determined exclusive of the stray capacitances, particularly between the leads feeding the plates.

For such measurements a model of the deflection system may be made, and grounded shields and guard electrodes placed at appropriate positions, particularly corresponding to the electron gun, to the outside of the cathode-ray tube, and to any other deflecting electrodes. The leads to the deflection plates should also be shielded from each other, so that the only capacitance measured between the two plates is that due to the space within which the beam deflection would take place [Fig. 2(a)].

Alternately, the factor c/ϵ_0 may readily be determined from a sketch of the equipotential lines and the lines of force in a cross section of the deflection plates. From Fig. 3, which shows the relative dimensions of the deflection plates of a type 5LP1 cathode-ray tube, 30 lines of force can be counted crossing the path of the electron beam. The difference of potential from plate to

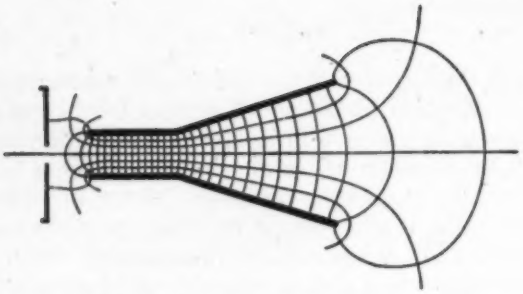

FIG. 3. (a) Electrostatic field of deflection plates.

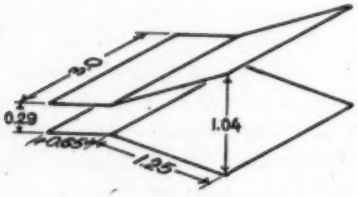

FIG. 3. (b) Dimensions of the plates in cm.

plate is 6 units. Thus

$$c=\rho/E=30\epsilon_0/6 \quad \text{or} \quad c/\epsilon_0=5.0.$$

The deflection angle for an acceleration potential V of 1000 volts is then

$$\theta/E=2.5\times10^{-3} \text{ radian/volt},$$

and for a distance of 250 mm from the deflection plates to the screen a sensitivity of 0.63 mm $-$kv/volt d.c. is obtained, which agrees favorably with the sensitivities of 0.60 and 0.67 mm/volt published by the manufacturers. The capacitances calculated from this are smaller than those specified for the same deflection system by the manufacturers, as the latter include the effects of considerable stray fields and the leads.

For a parallel-plate deflection system without edge effects, of axial length l and separation d, $c=\epsilon_0 l/d$ and there results

$$\theta=\frac{E}{2V}\frac{l}{d}, \tag{11}$$

the well-known formula for the deflection angle.[5] In order to take into account the edge effects of such a parallel-plate condenser,[6] it has sometimes been suggested to calculate an "equivalent" length of an idealized deflection system without fringing fields which would give the same deflection as the actual system. Instead, we have shown that the internal capacitance per unit width of the deflection system is the quantity which matters, and this by itself correctly includes all edge effects along the beam path. Lateral edge effects along the direction of the width of the plates do not play any part in the beam deflection. The factor c refers only to the middle section of the deflection plates, which is directly opposite to the beam.

Keeping in mind the assumption of constant beam velocity, it is seen from Eq. (9) that the deflection angle depends on the internal charge per unit width which can be placed on the system, and upon the potential accelerating the electron beam axially, regardless of the design of the deflection system or the voltage applied to it. A decrease of the accelerating potential at the deflection system[7] and an increase of the internal charge per unit width should be the aims pursued in designing either a new deflection system or an amplifier stage to supply it.

In order to show the distribution of the total charge q and the internal charge ρ between the total circuit capacitance C and the oscillograph deflection system, we may write

$$\rho=qc/C. \tag{12}$$

C here also includes the capacitance of the oscillograph deflection system to ground. For a given total charge q, the deflection angle can be made larger by making c as large compared to the total circuit capacitance as possible.

It has heretofore been suggested to make the deflection plate capacitance as small as possible. This analysis shows that, on the contrary, under these conditions the internal capacitance per unit width of the plates should be made as large as possible compared to the total circuit capacitance. This applies particularly when the oscillograph is connected to a circuit which already has some capacitance and which is supplied by a limited amount of charge q, as may be the case with ordinary vacuum tube amplifiers at high frequencies.

3. THE ARRANGEMENT OF THE DEFLECTION SYSTEM: USE OF A PARALLEL-WIRE LINE FOR DEFLECTION

The factor c/ϵ_0 is a dimensionless quantity unaffected by changes of scale, since both c and ϵ_0 have the same dimensions of farads per meter. From this it follows that deflection systems of the

[5] J. D. Cobine, *Gaseous Conductors* (McGraw-Hill Book Company, Inc., New York 1941), p. 553.
[6] J. T. McGregor-Morris and V. A. Hughes, J.I.E.E. **79**, 454 (1936).
[7] J. R. Pierce, Proc. I.R.E. **29**, 28 (1941).

same relative dimensions and shapes but of different over-all sizes will have the same deflection sensitivity as long as transit-time effects do not play a role. Thus, once the relative shape of a deflection system has been determined which has a sufficiently large capacitance c per unit width, those factors containing absolute magnitudes such as manufacturing tolerances, beam thickness and the maximum transit-time of the electrons determine the size with which this system should be constructed.

In past years manufacturers have used for deflection of cathode-ray beams pairs of plates flared out at the end facing the screen. Their axial length, however, entails a considerable transit time. At very high frequencies the time of transit of the electrons through the deflecting field reduces the magnitude of the deflection unless it is smaller than a half-period of the highest frequency to be used.[8,9]

Furthermore, in many tubes the leads from these plates are taken out of the tube at the base, which entails long leads with a considerable inductance and capacitance. Since this restricts the highest frequency which can be used with such an arrangement, the manufacturer's trend has been to bring the plates out directly at the neck of the tube, thus considerably reducing the lead inductance and capacitance. At very high frequencies, however, the lumped capacitance of the deflection plates and the lead inductance still produce undesirable resonance effects. At frequencies ranging far above several megacycles, the shunt capacitance of the output amplifier supplying the oscillograph has so low an impedance that no significant amplification can be obtained without a considerable supply of power. Thus, measurements at such high frequencies are frequently made by direct connection of the oscillograph deflection system to the voltages to be observed. But this presupposes a sufficiently high deflection sensitivity, or large enough voltages. However, with direct connection, the capacitance of the deflection system may have an undesirable shunting and detuning effect on the circuit to be measured.

Both the transit time and the capacitive shunting effect can be substantially reduced by

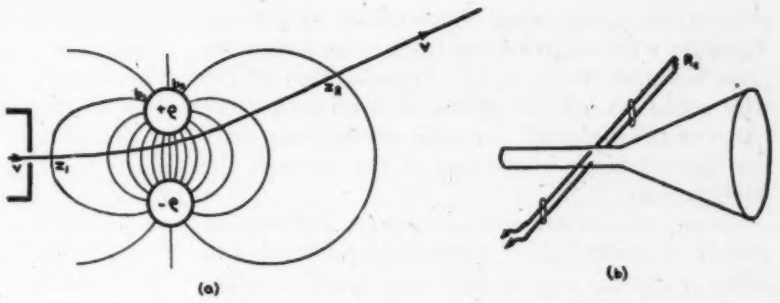

FIG. 4. Parallel-wire deflection sustem.

the same means, namely by using a closely spaced parallel-wire line as the deflection system arranged perpendicular to the electron beam (Fig. 4).

Since the capacitance per unit length of a parallel-wire line is[10]

$$c=\pi\epsilon_0/\cosh^{-1}(d/2r), \tag{13}$$

where r is the radius of the wires and d their spacing, then the deflection angle is, by Eq. (10),

$$\theta=\frac{E}{2V}\frac{\pi}{\cosh^{-1}(d/2r)}\simeq\frac{E}{2V}\frac{\pi}{\ln(d/r)}, \tag{14}$$

the last expression being valid for large values of d/r.

In this case the electrostatic field is mainly concentrated within a space between the wires as wide as their distance apart. Thus it can be shown that the significant part of the transit time is the time required by the beam to cross a space of the order of magnitude of the wire spacing.

As the wire spacing may be relatively close, the transit time will also be small. The voltage deflection sensitivity, although less than that of conventional deflection systems, due to the small capacitance c of the wire system, will still be sufficient for many applications.

As an example the case of parallel wires of 3-mm diameter, separated by 3 mm, shown in Fig. 4, can be compared to the deflection system of Fig. 3. The center-to-center spacing of the wires d is thus 6 mm, giving a value of $\cosh^{-1}(d/2r)=1.32$. Thus we obtain with the same screen distance of 250 mm a sensitivity of 0.3 mm kv/volt d.c., about half of that of the deflection plates described above.

This parallel wire deflection system has a

[8] L. L. Libby, Electronics **9**, No. 9, 15 (1936).
[9] H. E. Hollmann, Proc. I.R.E. **28**, 213 (1940).

[10] G. P. Harnwell, *Principles of Electricity and Electromagnetism* (McGraw-Hill Book Company, Inc., New York, 1938), p. 40.

characteristic resistance of 160 ohms. As a 3-mm diameter wire might be too thick to seal into the glass walls of the tube, the cross section of the wire could be reduced there, thus offsetting the effect of the dielectric constant of the glass upon the characteristic impedance of the wires at the lead-through.

Owing to the compactness of such a deflection system of parallel wires, the stray capacitances to other electrodes may be kept very small. In spite of the small value of c its ratio to these stray capacitances will be large.

Two additional advantages can be realized by using parallel wires for the deflection of the electron beam. First, many measurements at ultra-high frequencies for which oscillographs might be used are made at fixed frequencies, so that the parallel wires may be tuned like a Lecher line. Then, by proper adjustment of the tuning, a voltage maximum on the line may be adjusted to occur at the place where the electron beam travels between the wires. Owing to the high Q of such a line, very high maxima of charge and voltage may be obtained, thus ensuring a maximum deflection.

Secondly, for wide-band operation, the deflection wire system may be terminated at one end by its characteristic or surge resistance.[11] Naturally, a much greater input power to the line will be necessary for satisfactory deflection of the electron beam. However, the input impedance to the deflection system will be a pure resistance at all frequencies. For such a non-resonant line, the characteristic surge impedance is

$$R_c = 120 \cosh^{-1} (d/2r) \text{ ohms.} \qquad (16)$$

Thus the deflection in terms of the input current $I = E/R_c$ to the parallel-wire line is given by

$$\theta = 60\pi I/V, \qquad (17)$$

independent of the relative spacing d/r of the two wires. We see again that, corresponding to Eq. (9), the deflection angle is primarily determined by the current or charge on the two wires.

The power needed to drive this deflection system is lost in the terminating resistance, and is least when the characteristic impedance of the line is smallest. This requires thick wires with close spacing. The power needed to drive the line is independent of the frequency to be used. Contrasted with this is the case of conventional deflection plates, which for a given voltage draw a reactive power proportional to the frequency. Particularly for the study of transients, the absence of reflections obtainable by proper termination of a deflection line will be of advantage, since conventional deflection plates and their leads may introduce undesirable resonances into such transients.

If amplification of the deflecting signals should be necessary, special amplifier tubes with inherently low effective output capacitances must be used in order to utilize fully the wide-band features of an oscillograph deflection system using non-resonant parallel-wire lines.

Another advantage of parallel-wire deflection system is the small coefficient of coupling to the second pair of deflection plates or wires in the oscillograph owing to the small spacing of the two wires of the line. This reduces mutual stray voltages, which would produce spurious patterns.

4. CONCLUSION

Under the assumption of constant velocity of an electron beam and up to the range of significance of the transit-time effect, the factor governing the voltage deflection sensitivity of any arbitrarily shaped electrostatic deflection system is its internal capacitance per unit width. This includes the edge effects at the entrance and exit of the electron beam from the deflecting field and allows a static determination of the sensitivity by capacitance measurements, or a determination by mapping the electrostatic field of the deflection system. The absolute deflection of the beam depends on the internal charge placed within unit width of the deflection system.

A closely spaced parallel-wire line can be used to advantage as deflection system, if a low transit-time error is required. This provides means for absolute voltage measurements at very high frequencies. Large deflection angles may be obtained by a small input power if the deflection line is tuned to resonance. Where much power is available, the deflection line may be terminated by its characteristic impedance and will present a constant input resistance at all frequencies, making such a system useful for wide-band operation and the observation of transients.

The writer wishes to express his thanks to those members of the faculty at this laboratory who have reviewed this paper, and to the Allen B. Dumont Company for supplying the data on one of their cathode-ray tubes.

[11] W. Graffunder Hoc.-tech. u. Elek.-akus. **60**, 145 (1942).

A Novel Form of Refrigerator

J. R. ROEBUCK
Department of Physics, The University of Wisconsin, Madison, Wisconsin

(Received December 18, 1944)

When a gas is allowed to flow out along the radius in a rapidly rotating enclosure, it is compressed and therefore heated. The enclosure may be supplied with a coil of pipe carrying a cooling liquid to remove the heat of compression as formed in the gas. On guiding the gas back to the axis, it is cooled by its own expansion, and a maximum ΔT of about 150°C occurs. The work of expansion is determined by the rotor demand, not by the gas temperature or by the gas volume change. Both warm and cold fluids enter and leave the enclosure axially. Analysis shows that the cooling, ΔT, is given by $\omega^2 r^2/2C_p$. The rotational energy of the enclosure is not drawn upon by the steady fluid flows. The cooling liquid moves convectively through its circuit but the gas must enter the enclosure at a pressure somewhat above that at exit. A possible mechanical design is sketched. Maximum peripheral speeds allow 19 cal./gram to be extracted from the gas flow giving for air a drop of 77°C from room temperature. This is more than sufficient for most commercial refrigeration. Use of a favorable gas in the rotor gives sufficient ΔT to be very effective in gas liquefaction. Rotors may have their flows in series to increase the ΔT, and the gas may be at a supercritical pressure to keep it homogenous till released from the pressure. The device is expected to have high efficiency as a refrigerator. By utilizing the rejected heat, as Kelvin suggested, the device may be used for domestic heating.

1. INTRODUCTION

IN the early development of mechanical refrigeration, the compression-cooling-expansion cycle using air as working fluid occupied an important place. But for a variety of reasons it has been displaced by the somewhat similar cycle employing liquid-vapor as working material, especially for relatively small temperature drops while for large temperature drops, as for example in liquefying air, gas is still used for the working material.

In the theoretical discussion accompanying the early experimental work, Kelvin pointed out the dominating advantage, in the heat theory, of an engine applying the Carnot cycle. The practical application is, however, faced with serious difficulty, among which may be noted the complete failure of all attempts to compress a gas isothermally in any reasonable time. The corresponding problem of expanding the gas adiabatically has been only partially met in the uniflow expansion engines. The bulky machines for handling gas at atmospheric pressure magnify the overhead, the friction losses, and the conductive losses. The following scheme meets some of these difficulties in what appears to be a new way.

2. GENERAL THEORY

To study the behavior of the working material separate from the mechanical difficulties, suppose that the bent pipe (Fig. 1) *a b c d e f* of strong nonconducting material, may be rotated in the bearings *B* and *B* at any desired very high speed.

Consider a flow of air adiabatically from *a* to *f*. As the air passes along *bc* out from the axis, it will be subjected to a centrifugal force toward *c* so compressing the air along *bc* and in *cd* to a pressure above that in *ab* and raising its temperature. As this compressed warmer air moves in toward the axis along *de*, it is progressively relieved of the centrifugal force and expands back to its former pressure and temperature by the time it enters *ef*.

Next let us supply the section *bc* with suitable cooling means so that the heat of compression along *bc* will be carried away. This compressed gas may thus approach *d* with approximately the same temperature as at *a* and will be strongly cooled by the adiabatic expansion along *de*. The resulting drop in temperature will depend on the ratio of the pressures at *d* and *e*, and on the character of the particular gas used. Under the most favorable circumstances it appears possible to obtain up to 150°C drop.*

It will be observed that the gas along *de*, being colder at corresponding radial points than the

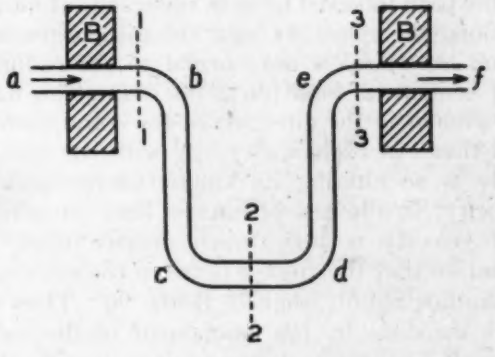

FIG. 1.

* J. W. Beams has observed some such cooling under quite similar circumstances. See *Science in Progress* (Yale University Press, 1940), edited by G. A. Baitsell, p. 246.

gas along *cb*, will be denser also. Thus under flowing conditions the pressure gradient along *de* will be larger than that along *bc* produced by the centrifugal force; and hence for flow to be maintained, the pressure in the gas at entry at *a* must be sufficiently greater than that at *f* to overcome this opposing pressure, and also of course to overcome any frictional effects in the gas flow. Moreover, the external work thus carried into the system may possibly satisfy the requirement of the second law for the expenditure of work to raise the heat from the temperature of the gas being cooled by expansion in the arm *de* to the temperature of the cooler in the arm *bc*.

This mechanical system thus consists of a compressor with concurrent abstraction of compressional heat in *bc*, and an adiabatic expansion engine in *de*. They are very directly coupled mechanically. In a *steady running state*, every gas particle in moving from *b* to *c* acquires a very large kinetic energy due to the large circumferential velocity. Along *cd* this kinetic energy does not change. But as the gas particle moves back toward the axis along *de*, it loses this energy to the tube. Since the number of particles in unit time moving outward across any cross section in *bc* must be exactly equal to the number moving inward across any cross section in *de*, the circumferential velocity energy of the gas makes no major demands on the rotary energy of the tube.

3. INTERCHANGE OF ENERGY BETWEEN PERIPHERAL VELOCITY AND RADIAL WORK

When a small body m at A in Fig. 2 is moved a distance dr inward along the radius r, the work $m\omega^2 r dr$ is done against the centrifugal force. If at the same time the radius is rotating about O, the path followed by m in the resultant motion is along the spiral AC and the displacement ds along the spiral is not normal to the radius r. The centripetal force along the radius now has a component in the direction of the spiral motion, and thus can exchange energy with the moving body m so altering its kinetic energy and its velocity. In the case of interest here the peripheral velocity is very much greater than the radial, so that the angle θ between the spiral and the radius is only slightly below 90°. Thus the work dw done by the component of the radial force, F, over the distance ds along the spiral is, $dw=(F\cos\theta)ds=Fdr=m\omega^2 r dr$. Thus the work done in the arm *de* (Fig. 1) by the gas pressure in moving the gas particle m against the centrifugal force, appears as work done in the direction of the spiral and will accelerate the angular velocity of *de* unless the energy is withdrawn elsewhere from the system. Conversely, the gas particle moving out the arm *bc* draws upon the peripheral kinetic energy of the system for (a) its needed increment of peripheral kinetic energy and (b) the energy needed to supply the work done by the centrifugal force along the radius, which work is spent in compressing the gas.

For the case of interest here the angular velocity, ω, is to be held constant by outside means. As m moves out the arm *bc* from the axis to the end of the radius, r, it acquires a peripheral kinetic energy of $\frac{1}{2}m\omega^2 r^2$ and has work done upon it by the centrifugal force of

$$\int_0^r m\omega^2 r\, dr=\tfrac{1}{2}m\omega^2 r^2,$$

so that m draws upon the energy of the rotating system, or upon its regulating energy store, for a quantity of energy $m\omega^2 r^2$.

Similarly in *de* the particle loses its peripheral kinetic energy, $\frac{1}{2}m\omega^2 r^2$, to the tube as it moves toward *e* against the force $m\omega^2 r$, against which it does also the work $\frac{1}{2}m\omega^2 r^2$, which work must be drawn from the enthalpy of the gas, as appears in Eq. (2). This loss of enthalpy occurs for purely mechanical reasons independent of whether or not the heat of compression has been abstracted in the arm *bc*. Only in case the kinetic energy (heat) of the particle falls below

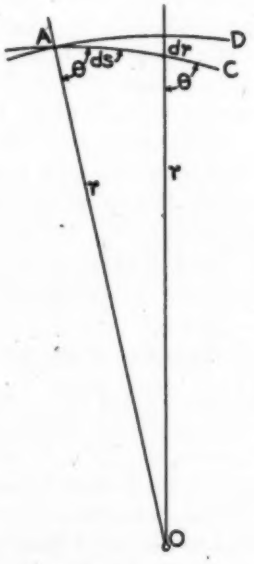

FIG. 2. Spiral path of gas particle.

the $\frac{1}{2}m\omega^2r^2$ will the demand fail to be met, in which case also the gas will fail to pass through the tube.

It thus appears, as also in the case of the peripheral velocity energy, that the radial work requirements in *bc* and in *ed* are set entirely by the rotation requirements, independent of the means for supplying or absorbing this work. That is, the radial work requirement at every radial point in *bc* is exactly matched at the corresponding radial point in *ed*. Since also the mass flow through every cross section of the tube *af* is the same in the steady flow state, it follows that the radial work requirement in *bc* is exactly equal and opposite to that in *de*, and hence that the radial work in the steady gas flow makes no net demand on the rotary energy of the system.

4. UNIQUE ASPECTS OF THIS EXPANSION ENGINE

The work done by the expanding gas is thus not set by the character of the (p, v, t) relations of the particular gas but by the demands of the rotating system; that is for the element of the gas to reach the axis this quantity of work must be supplied to the rotating system. This is a unique difference from all other types of expansion engines in which the falling of the pressure due to falling gas temperature lessens markedly the work extracted by the piston.

This situation, where a definite force can be exerted on each molecule of the working fluid without the immediate presence of solid bodies to accomplish it, allows of a second unique difference with all other types of compressive-expansive engines. The gas molecules may be made to move among surfaces cooled or warmed by a flow of liquid from the outside without interfering in any way with the work relations in the gas. Sufficient area of such surfaces with an ample flow of liquid will hold the temperature of the compressing or expanding gas as constant as that of the liquid. That is, the compression or expansion may be made closely isothermal. Conversely, the absence of such surfaces in a guide tube of poorly conducting walls allows the steadily flowing gas to bring the wall at each place into temperature equilibrium with the gas at that place, so providing nearly ideal conditions for adiabatic changes.

5. THERMODYNAMICAL RELATIONS

Consider the energy gains to and losses from the volume of the tube between cross sections *1*, *2*, and *3* in Fig. 1. Take account of those due to the gas flow and neglect those due to any heat exchanges through the tube wall. Express all the energy quantities in heat units. For unit mass transfer across *1*, the *gains* to the space between *1* and *2* are: (1) u_a = intrinsic energy coming with the gas in across *1*; (2) p_av_a = work done by the outside force in driving specific volume v_a in across *1*; (3) $\frac{1}{2}\omega^2r^2$ = work done by the tube to give peripheral velocity to the gas between *1* and *2*; (4) $\frac{1}{2}\omega^2r^2$ = work done by the centrifugal force on the unit mass between *1* and *2*. And for unit mass transfer across *2* from the space between *1* and *2*, the *losses* are: (5) u_c = intrinsic energy passing out with the gas across *2*; (6) p_cv_c = work done to force the specific volume v_c out; (7) $\frac{1}{2}\omega^2r^2$ = kinetic energy (peripheral) carried out with the gas; (8) q = heat carried away by the cooling liquid. It will be noted that (1) offsets (5) since the intrinsic energy of a gas is a very small function of the volume, and the temperature at *a* and *c* are alike; that (2) offsets (6) since $p_av_a = RT = p_cv_c$; (3) offsets (7); and therefore $\frac{1}{2}\omega^2r^2 = q$. It may be inferred that q is the work done in compressing the gas isothermally in *bc*, so that

$$q = \tfrac{1}{2}\omega^2r^2 = \int_{v_c}^{v_a} p\,dv = RT_c \log_e (v_a/v_c) = RT_c \log_e (p_c/p_a). \quad (1)$$

That this relation follows from the steady state conditions for the gas in the rotating arm *bc* will be shown below.

Similarly, consider the energy gains and losses to the volume of the tube between *2* and *3*. For unit mass transfer in across *2*, the *gains* are: (1) u_c = intrinsic energy entering with unit mass across *2*; (2) p_cv_c = work done to force the specific volume in; (3) $\frac{1}{2}\omega^2r^2$ = peripheral kinetic energy entering with the gas; (4) $q = 0$ since there is no heat input to offset the expansion work. And for unit mass transfer out across *3*, the *losses* are: (5) u_e = intrinsic energy passing out with the gas across *3*; (6) p_ev_e = work done to force the specific volume out; (7) $\frac{1}{2}\omega^2r^2$ = peripheral kinetic energy transferred to the tube between *2* and *3*; (8) $\frac{1}{2}\omega^2r^2$ = work done by the gas against the radial force between *2* and *3*.

Again it will be noted that (3) offsets (7), and hence on the basis of the conservation of energy,

$$(p_cv_c - p_ev_e) + (u_c - u_e) - \tfrac{1}{2}\omega^2r^2 = 0,$$

$$R(T_c - T_e) + C_v(T_c - T_e) = \tfrac{1}{2}\omega^2r^2,$$

and

$$C_p(T_c - T_e) = \tfrac{1}{2}\omega^2r^2, \quad (2)$$

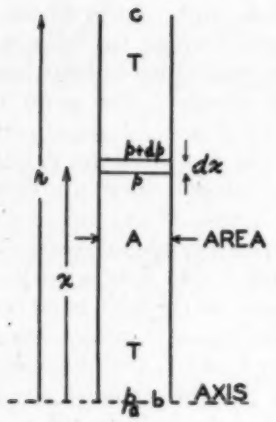

FIG. 3. Steady state in arm *bc*.

since the general gas law $pv=RT$ holds. Since *enthalpy* is defined as $(u+pv)$ and the first equation may be rewritten as

$$(u_c+p_cv_c)-(u_e+p_ev_e)=\tfrac{1}{2}\omega^2r^2,$$

we note that the change in the enthalpy of the gas between the points c and e is $\frac{1}{2}\omega^2r^2$.

In this situation, T_c, ω, and r are chosen for the experiment, C_p is fixed by the choice of working gas, so that T_e can be calculated from Eq. (2).

From the adiabatic and the general gas laws it is readily shown that

$$T_c/T_e=(p_c/p_e)^{(K-1)/K} \tag{3}$$

where $K=C_p/C_v$. If the discharge pressure p_e be chosen, p_c may be calculated from Eq. (3). This p_c may then be used in Eq. (1) for isothermal compression to give p_a.

In case the gas used does not obey the simple gas laws sufficiently well, and if the gas has been sufficiently well measured to have available engineering charts, these charts may be readily used to carry out the above calculations with closer correspondence to the behavior of the particular gas.

6. WORK RELATIONS IN THE ARMS *bc* AND *de* IN THE STEADY STATE

It will next be shown that Eq. (1) is satisfied when steady state flow conditions have been established in the isothermal arm *bc* as it is rotated at constant angular velocity ω. Under these established conditions in the arm *bc*, Fig. 3, consider a layer of small thickness dx fixed at an arbitrary radial position x in *bc*. The pressure drop dp across dx, and the density ρ of the layer have become constant, although a constant stream of molecules passes through dx. The mass in the layer has also become constant at $\rho A dx$. Since the layer is constrained to rotate with the tube, it is subject to the centrifugal force $(\rho A dx)\omega^2x$. The mass of this layer is in equilibrium when this centrifugal force is just balanced by the difference of the bombarding forces on the two faces, so that

$$A(p+dp)-A(p)=Adp=\omega^2x\rho A dx,$$

$$\omega^2xdx=dp/\rho=RT_a(dp/p). \tag{4}$$

Since ω and T_a are constants, integration gives

$$\tfrac{1}{2}\omega^2x^2=RT_a\log_e(p_x/p_a), \tag{5}$$

holding for any point x in the rotating tube. When $x=r$,

$$\tfrac{1}{2}\omega^2r=RT_a\log_e(p_c/p_a). \tag{1}$$

The right-hand member may be recognized as the work required to compress the gas isothermally from the pressure p_a to p_c which work is converted into the heat of compression q. All of which confirms the conclusions in the discussion of Eq. (1) above.

A similar argument may be based upon Eq. (4) for the *adiabatic* expansion in the arm *de*, Fig. 1. It can thus be shown that the steady state distribution is satisfied by the conditions of Eqs. (2) and (3).

7. THE GAS CYCLE

The gas cycle involved in this process may be described as in Fig. 4 by a pv diagram which is here drawn to scale in arbitrary units. The condition of the gas at the starting point α is set by its pressure $p_\alpha=p_e$ and its temperature T_a. The pressure p_α is raised to p_β by the auxiliary compressor which process is here assumed as isothermal and $T_a=T_\alpha=T_\beta=T_\gamma$. The pressure $p_\beta=p_a$ is raised to $p_\gamma=p_c$ in the rotor, Fig. 1, *bc*, under reasonably isothermal conditions. The pressure is dropped in the adiabatic expansion $\gamma\delta$ all the way back to p_α and the temperature T_a drops to T_e. The gas is warmed at constant pressure p_e, from T_e back to T_a, completing the cycle.

The two stages $\alpha\beta$ and $\beta\gamma$ form a continuous curve in Fig. 4, being continuous in pressure and in volume, and really form one step, even though the work for each is supplied separately and the heats of compression are disposed of separately.

The net external work done per cycle on the system is given by the area $\alpha\beta\gamma\delta$, and the

TABLE I.

No.	Gas	Molec. Weight	c_p g.cal/ g.deg	F.P.	B.P.	q g.cal.	$-\Delta t = t_e - t_a$	t_a	t_e	P_a atmos.	P_e atmos.	P_s atmos.	E	E'
1	Air[1]	28.8	0.248		−190°C	19.1	79.0	20°C	−59°C	1.2	3.4	1	5.71	2.71
2	Air[1]					19.1	81	20°C	−60°C	12.3	30	10		
3	Air[1]					19.1	81	−39°C	−120°C	1.4	4.8	1		
4	Air[1]					19.1	80	−25°C	−105°C	1.4	4.4	1	3.40	2.10
5	Air[1]					19.1	85	−105°C	−190°C	2.8	13	1	1.52	0.98
6	Air[1]					38.2	173	−17°C	−190°C	6.9	52	1		
7	Argon	39.9	0.123	−189.2°C	−185.7°C	19.1	155	−30°C	−185°C	2.75	14	1		
8	Neon	20.2	0.246	24.6°K	27.3°K	12.3	50	77.2°K	27.3°K					
9	Hydrogen[3]	2.0	3.42	14.2°K	20.35°K	19.1	8.6	29°K	20.4°K	1.25	2.5	1		
10	Helium[2]	4.0	1.24	1.3°K	4.21°K	19.1	14.4	34.8°K	20.4°K	1.30	3.4	1		
11	Helium[2]					19.1	17.3	21.5°K	4.2°K	14	62	1		

[1] H. Hausen, *Der Thomson-Joule Effect* (Forschungsarbeiten von verein Deutscher Eng. 1926), Vol. 274.
[2] Keesom and Houthoff, Comm. of Leiden Lab. (Supp. No. 65e, 1928).
[3] Keesom and Houthoff, Comm. of Leiden Lab. (Supp. No. 65d, 1928).

position of β on $\alpha\gamma$ is to be so chosen that the compression $\alpha\beta$ supplies this net external work. So that

$$RT_a \log_e \frac{p_\gamma}{p_\alpha} - C_v(T_a - T_e) - p_e(v_a - v_\delta) = RT_a \log_e (p_\beta/p_a),$$

$$RT_a \log_e \frac{p_\gamma}{p_\alpha} - RT_a \log_e \frac{p_\beta}{p_a} = C_v(T_a - T_e) + R(T_a - T_e),$$

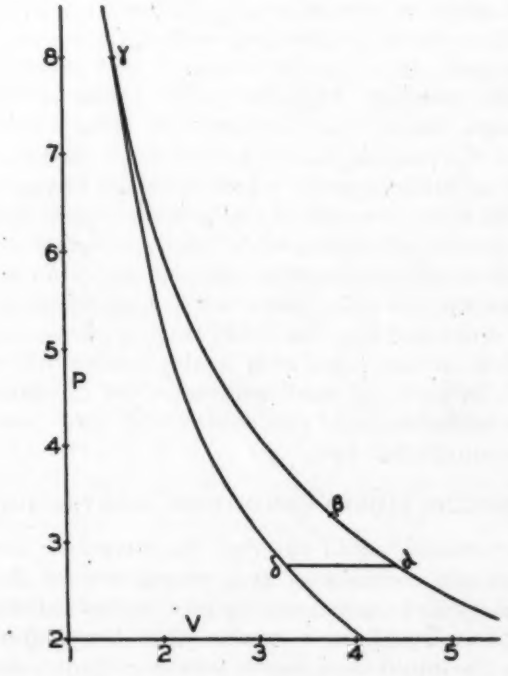

FIG. 4. Gas cycle.

and

$$RT_a \log_e \frac{p_\gamma}{p_\beta} = C_p(T_a - T_e) = \tfrac{1}{2}r^2\omega^2 \qquad (6)$$

which checks with Eqs. (1) and (2). Moreover, inserting the values from line 1, Table I, and solving for p_β checks with the value there obtained from the engineering charts for air.

8. EFFICIENCY

The refrigeration efficiency, E, is, therefore,

$$E = \frac{\text{total heat energy abstracted}}{\text{net external work supplied}} = \frac{RT_a \log_e (p_\gamma/p_\beta)}{RT_a \log_e (p_\beta/p_a)} = \frac{\log_e (p_\gamma/p_\beta)}{\log_e (p_\beta/p_a)}. \qquad (7)$$

The refrigeration efficiency of a reversed Carnot cycle may similarly be expressed as

$$E' = \frac{Q_2}{W} = \frac{Q_2}{Q_1 - Q_2} = \frac{T_2}{T_1 - T_2}. \qquad (8)$$

Before applying this to the rotor it is to be noted that for E', all the heat Q_2 must be lifted from T_2, where it is absorbed, to T_1, where it is discharged. In the rotor, however, while all the gas drops from T_a to T_e, the heat is not all raised from T_e to T_a. If an element of gas, dm, be followed down de, Fig. 1, it will be observed to lose heat steadily and continuously all the way, each loss in enthalpy, dq, being then and there converted into work and handed to the tube de. This work is transmitted by force transmission through the rigid tube to the part bc where it supplies the heat of compression which

is discharged to the cooling water at T_a. Thus the heat is being lifted at every point and from every temperature along *de*, to be all discharged at the temperature T_a in *bc*.

To apply this Carnot refrigeration efficiency E', we have

$$dq = E'dw = [T_2/(T_1 - T_2)]dw,$$

where dw is the work necessary to lift the heat dq from T_2 to T_1. The relation between dq and dt is given by $dq = C_p dt$, hence,

$$dw = [(T_1 - T_2)/T_2]dq = C_p[(T_1 - T_2)/T_2]dT_2,$$

where the integral is to be taken with T_1 fixed at T_a and T_2 varying from $T_1 = T_a$ down to the limit $T_2 = T_e$. Therefore inserting these special variables, we have

$$-w = -\int_{T_a}^{T_e} C_p\left(\frac{T_a}{T} - 1\right)dT$$

$$= C_p T_a \log_e \frac{T_a}{T_e} - C_p(T_a - T_e).$$

In the adiabatic expansion, to which this may now be applied, the states are characterized thus:

Initial state $T_a p_\gamma \quad v_\gamma$

Final state $T_e p_a \quad v_\beta$

$$\therefore \quad \frac{T_a}{T_e} = \left(\frac{p_\gamma}{p_a}\right)^{(K-1)/K} = \left(\frac{p_\gamma}{p_a}\right)^{R/C_p},$$

$$\therefore \quad -w = C_p T_a \frac{R}{C_p} \log_e \frac{p_\gamma}{p_a} - C_p(T_a - T_e)$$

$$= RT_a \log_e \frac{p_\gamma}{p_\beta} + RT_a \log_e \frac{p_\beta}{p_a} - C_p(T_a - T_e)$$

$$= RT_a \log_e \frac{p_\beta}{p_a}.$$

Here w is the net external work, supplied to the cycle, calculated as necessary by applying the Carnot refrigeration efficiency to the heat as it is raised to the discharge temperature. This net external work is the same as that which appears in Eq. (7) and so gives the same value of the efficiency.

Hence it is now proved that the external work supplied by the auxiliary compressor in raising the pressure from p_e to p_a supplies the quantity of external work necessary to raise the temperature of the discharged heat to the temperature of the cooling fluid in the rotor, so satisfying the demands of the Second Law.

That the efficiency, E, Eq. (7), obtained in the rotor is decidedly better than E' as defined in Eq. (8), may be readily appreciated from the two sets of circumstances involved. E' corresponds to the cooling of a fluid-flow by a boiling liquid as commonly practiced. In comparison with this, it is to be noted that the cooling in an ideal exchanger, as in $\delta\alpha$ of Fig. 4, is assumed to have unit efficiency. The values of E and of E' for some cases are given in Table I, where the E's are pure numbers, that is, the heat discharged and the work expanded are both expressed in the same energy unit. The advantage of E over E' is very material.

9. REVERSIBILITY

This rotor process as described above is close to thermodynamically reversible. If, with all the conditions of pressure, temperature, and flow as described, the pressure supplied at *a*, Fig. 1, is alone decreased a little, the flow of gas will reverse going now from *f* toward *a*, compressing adiabatically from *e* to *d*, and expanding isothermally with absorption of heat from *c* to *b*, and delivering the gas at *a* at a pressure raised above that of *f*, so converting some heat into work. If now with suitable reservoirs of gas at *d* and at *f* to maintain this reversed flow, the fluid entry temperature at *a* be raised a little, the flow will be accelerated, so that the pressure previously at *a* may be restored, and the flow remain reversed. Thus by manipulation of the pressure (work) and temperature (heat) variables, the process may be run in either direction with, it would appear, relatively small changes.

This ready reversal of the process means that its "intrinsically irreversible" steps are relatively unimportant, that specifically the heat transfer by conduction takes place with small temperature drops and that the small friction allows the gas flow to take place with small pressure drops. That, in fact, the rotor process is not far from "thermodynamically reversible" and hence correspondingly efficient.

10. COOLING LIQUID CONDITIONS. CONVECTION

The cooling liquid entering the rotor near the axis is also compressed as it moves toward the periphery and expanded as it returns toward the axis. Since liquids are normally much denser than gases, the liquid used rises in pressure toward the periphery much more than the gas. The liquid

should on this account be contained in very strong walled tubes of rather small diameter wound in cylindrical layers, with the gas moving among the tubes. Liquids also change their temperature on compression, rising in temperature if the coefficient of volume expansion is positive. These temperature changes are very much smaller than those for gases—a fact which makes this rotor device feasible. Thus, for the change of about 400 atmos. to be expected at the limiting linear peripheral velocity, water initially at 20° rises less than 1°C, and organic liquids 2°–7°C. Water is unlikely to be used in the range of negative expansion coefficient since the convective force will oppose the cooling flow and, even though it is apparently possible, to achieve a small total drop in temperature for the pressure change of 400 atmos. Gases differ considerably in their temperature changes on the same adiabatic compression, but these differences are difficult to employ for such cooling purposes as are needed here.

For the liquid to cool the gas most effectively, the two flows should probably run countercurrent. Hence, the liquid entering on the axis should proceed directly to the periphery out of contact with the gas and return to the axis under the best possible contact with the compressing gas. If the heat absorbed raises the temperature and expands the liquid, the column of liquid returning to the axis becomes less dense than that going to the periphery. The two radial columns become unbalanced in the large artificial gravity field, producing a very considerable pressure difference which drives the liquid around its circuit. The work necessary for this drive, as in ordinary convective flows, is drawn from the heat energy causing the expansion. This makes unnecessary any other means for circulating the liquid and at the same time does not draw on the rotary energy. As the heat to be absorbed is increased, the tendency for the liquid temperature to rise will be largely offset by the increase in driving pressure difference increasing the mass flow of the liquid. This flow is thus quite self-regulating, changing roughly proportionally to the mass flow of gas through the rotor.

11. GAS CONVECTION

A somewhat similar convective situation is present in the gas flow. If a small volume of gas loses heat by contact with the tubes carrying the liquid, its density increases, throwing it out of equilibrium with its surrounding gas. This cooled

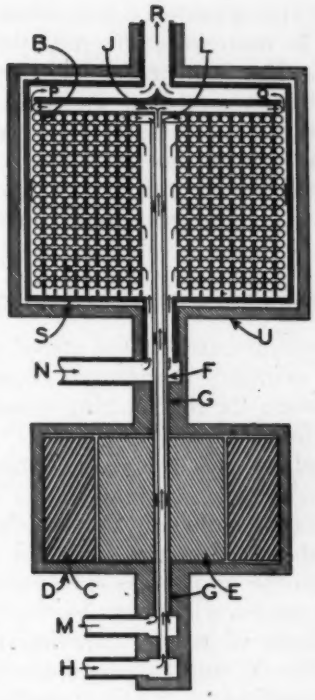

FIG. 5.

gas is accelerated by the large artificial gravity out the radius and hence up the pressure gradient. This movement ceases when the compressional heating brings this cooled gas back into equilibrium with its new surroundings. Such movements setting up heavy convection in the gas greatly facilitate the transfer of heat between the gas and the liquid. If any radial channel in the gas has no effective means of losing its heat of compression while parallel neighboring channels have, the gas in the former channel will lie effectively quiescent while the movement takes place in the cooled channels. Hence in the design there is no need to be extremely particular to avoid any such channels, since very little flow will take place there.

12. REFRIGERATION PROCESS IS INDEPENDENT OF ROTARY ENERGY OF ROTOR

From the discussions above, it would appear that after a steady state has been reached in the operation of the rotor, the rotor drive will not be called upon to supply any major quantities of energy on account of the flows. Energy for driving the gas and liquid flows are separately supplied, the gas from the raised inlet pressure and the liquid from the heat absorbed. Rotary energy is lost in bearing friction and in gas

friction on the outside of the rotor, but these should not be materially affected by the gas and liquid flows. Neither the gas nor the liquid can leave the rotor exactly on the axis, so that in each a small escape of rotational energy in the form of fluid turbulence will occur. Except in such minor ways, the refrigeration process does not draw upon the rotational energy of the rotor.

13. DESIGN OF ROTOR UNIT

The considerations detailed above, when combined with ordinary mechanical considerations, lead to a design for the rotating vessel as represented diagrammatically in Fig. 5.

The cylindrical case S is made of the strongest available metal, e.g., chrome nickel steel, with a wall thickness sufficient that the stress from the internal gas pressure will not add very materially to the unit stress. The stress limiting the angular speed will occur in this wall or in the outer layer of tubing carrying the liquid. This cylinder S rotates about its axis with moderate clearances in a heavy steel cylinder U which will serve as a guard against flying parts in case of trouble and also permit S to rotate in a partial vacuum. S is carried on the entrance and exit tubes, a convenient one of which may be used to drive it.

Since for any effective use the speeds required are high, it will be desirable that the driving power have a very fixed upper speed limit such as a synchronous motor or any induction motor driven by high frequency electrical power. Since, as indicated above in the theory, the power demand from this rotor by the process is small, the size of this motor will be set partly by the time required to bring the rotor up to its working speed.

C and E of Fig. 5 are intended to illustrate a high frequency induction motor. The field magnets of the stator C are mounted inside the steel case D, and the squirrel cage rotor E is carried directly on the cooling-fluid exit pipe F running in the bearings G and G.

The cooling fluid—water, alcohol, or other light mobile fluid—enters the apparatus at H, the rotating inlet tube at I, and divides at the manifold J for the represented case into 8 strands. These proceed to the periphery directly where they are wound as 8 parallel strands in a single layer on the perforated steel cylinder B. These perforations are narrow slots running circumferentially for rather short angular distances.

The 8 tubes coming from the manifold J and wound parallel on the cylinder B pass over the lower end edge of this cylinder to be wound back to the upper end on the next inner cylinder. These tubes are so wound and the cylinders shrunk on them as to make a very rigid strong assembly. The tubes are suitably spaced to allow effective gas flow among them and are provided several times per circumference with septa parallel to the axis and to the radius so that the gas will always move around with the same angular speed as the rotor. These septa are formed by inserting between the tubes during winding pieces of metal shaped to fit the spaces between adjacent tubes of one layer and between successive cylinders. The tubes finally reach the manifold at L and join the liquid outflow tube, to leave the rotor at M.

The compressed gas enters at N, passes along the axis, spreads out among the tubes, gathers along the periphery, to pass over the edge of the disk PQ, to move in to the exit at R on the axis. The space between P and Q has a number of radial-axial septa to assure that the gas has always the same angular velocity as the rotor.

It is to be noted that the tube layers at successively greater coil diameters run at successively smaller angles to the plane normal to the axis. Also that the slots cut in the cylinders between these tube layers should for maximum strength be cut parallel to this plane. Hence it is not possible by any choice of plane of section to present a clear picture of the gas flow pattern among these tubes.

It will, however, be evident that the gas flows parallel to the pipes in each layer for small angular distances between steps from one layer to the next. If these angular distances be kept alike, the linear distances involved increase with the radius. Since the work done in compressing the gas along the radius increases proportionally with the radius, the heat to be transferred per unit area of tube remains the same. Since the gas density increases with radius, the gas velocity past the adjacent metal parts decreases in successive layers toward the periphery. Moreover, the huge artificial gravity field greatly exaggerates convective movement in the gas. The cooling surfaces on the tubes are thus swept by movement of the surface gas layer, and the heat exchange is greatly accelerated. The mass contact of the gas and its convective momement combine to make the heat exchange very effective.

14. ROTATIONAL SPEED LIMIT

The highest peripheral linear speed at which a machine like this may be run without failure sets the limit on the energy extraction from unit mass of gas. As long as this peripheral linear speed is kept unchanged, the diameter and length of the rotor may be determined by the desired gas flow. Analysis also shows easily that for constant peripheral linear speed the effect of the radial size of the rotor on its strength may be disregarded in a good first approximation. Stodola[1] in his treatise on turbines lays down this limit very emphatically at 1300 ft./sec. (4×10^4 cm/sec.) for the highest tensile strength steels. Beams[2] working with high speed centrifuges says that 8×10^4 cm/sec. is possible. Stodola's limit which may reasonably be used here leads to an energy extraction of 19.1 cal./gram. Since this quantity goes up with the square of the speed, Beam's limit, which experience may show feasible, gives 76 cal./gram.

15. CONTROL OF WORKING RANGE OF TEMPERATURE

It is evident from the above that the temperature range over which the rotor will lift heat depends first upon the gas chosen (the smaller its specific heat, the larger the step) and second upon the linear peripheral velocity given the rotor. Following the choice of working gas, the peripheral velocity can be adjusted to give the desired temperature step. Unfortunately the refrigerating capacity falls in the same proportion as the temperature step when the peripheral speed is reduced.

It is possible, however, to maintain the capacity of the machine but to fix the drop in temperature economically at less than its full drop. The part of the rotor, PQ as described in Fig. 5, in which the expansion to the axis takes place, will be increased in axial length to receive a coil like that in the compressional part. The outer diameter of this coil will however coincide with the place in the adiabatic expansion where the gas temperature becomes equal to the outlet temperature desired. A liquid to be cooled is circulated through the pipes of this coil by an outside pump as the convective situation opposes the flow. The heat so supplied to the expanding gas, continues to be drawn on for the further isothermal work, but the gas temperature is not allowed to fall materially further. The work required to carry the gas back to the axis is unaffected, and the resulting quantity of heat extracted is also unaffected. But because of the higher average temperature along this expanding column, the average density remains less than when the full adiabatic expansion takes place. Hence the pressure required to drive the gas through the rotor is lessened. This is in agreement with the Second Law in requiring less external work to lift the heat up a smaller temperature step. It should also be noted that the gas escaping from the rotor is below its inlet temperature and is available also for cooling.

16. USE OF COLD GAS TO PRODUCE LIQUID

The normal product of the rotor is a homogeneous gas, A, cooled materially below its rotor entry temperature. If A's low temperature lies a few degrees above or below the normal boiling temperature of a second gas, B, then pass the first gas A through an exchanger counter-current to a flow of B compressed well above its critical temperature. The compressed B cools as a homogeneous fluid of nearly constant but raised specific heat which after expansion at a valve will be almost completely liquid. The flows of A and B, for economical running, will need to be so adjusted that B in dropping to the entry temperature of A will give up just enough heat to raise A to the entry temperature of B. If B can be cooled below its normal boiling temperature enough that the usual liquid Joule-Thomson warming just brings it to its boiling temperature, the whole of B will become liquid. In case it is difficult to cool B quite that much, it will cool itself by boiling, and its cold vapor may be used to cool more compressed B. The work cost of compressing B, if done isothermally and reversibly, counts entirely as part of the necessary work cost of liquefying B. This is effected (a) by lessening the enthalpy which must be extracted to reduce B to a liquid and (b) by raising the temperature at which this enthalpy may be taken from B. Incidentally, the compression has spread the heat of condensation over a wide and raised temperature range where it appears through an increase in the specific heat.

17. WORKING GASES

In Table I are listed a group of gases of interest for use in this rotor. Engineering charts based on their measured physical properties are avail-

[1] Stodola, *Steam and Gas Turbines* (McGraw-Hill Book Company, Inc., New York, 1927), p. 240. Translated by L. C. Lowenstien.

[2] J. W. Beams, Rev. Mod. Phys. **10**, 260 (1938).

able for three of them. To use these charts recall the equation two lines above Eq. (2), namely

$$(p_c v_c - p_e v_e) + (u_c - u_e) = \tfrac{1}{2}\omega^2 r^2$$

or

$$h_c - h_e = \Delta h = \tfrac{1}{2}\omega^2 r^2 \qquad (9)$$

where $h = u + pv$ = enthalpy.

Consider the rotor process in the reverse direction to which it actually is used. The adiabatic expansion is isentropic being reversible and exchanging no entropy with the outside. Choose the delivery pressure p_e and guess t_e or calculate it approximately as in Section 5 on the assumption of the gas laws. Locate $p_e t_e$ on the chart and move along a line of constant entropy a distance given by Δh of Eq. (9). If the point reached does not leave the chosen t_c, shift the assumed t_e until it does. Thus read p_c, t_c, and S_c.

From this point, $t_c p_c S_c$, consider an isothermal expansion where the S increases by an amount h/T_c. This gives p_a. The numbers in the right hand part of Table I were obtained by these methods except for argon and neon for which usable charts were not available. The subscripts refer to Fig. 1.

The cooling of 79° in line 1 is more than sufficient for most commercial uses in the storing and handling of food, whether frozen or not. The power savings should be very material for the large installations, particularly for the manufacture of ice. The refrigeration capacity of a rotor could probably be increased materially by working from a base pressure P_e of 10 atmos. as computed for line 2 of the table, instead of a P_e of 1 atmos. as in line 1.

18. AIR LIQUEFACTION

For the writer, the greatest interest in the use of the rotor comes in the field of deep refrigeration, for example, as in the liquefaction of gases, particularly of air. Most air liquefaction processes used commercially employ precooling, as for, example, with the usual liquid-vapor carbon dioxide cycle, yielding down to approximately −50°C. In line 3 of Table I air at −39°C will suffer about the same 79°C drop by passing through the rotor. The inlet pressure p_a steps up a little due in part to the decreased specific volume of air at −39°C and in part to the decrease in the thermodynamic efficiency of the refrigeration cycle at the lower temperature. The Hylandt process uses a considerable fraction of its air supply after compression to 200 atmos. to provide a precooling to −120°C for the remainder, the power cost of which is much greater than for that outlined above.

A more effective arrangement, however, is that covered by lines 4 and 5 using two rotors in series following a carbon dioxide precooler. The carbon dioxide cools the inlet air and cooling liquid to −25° for the first rotor. Its outlet air at −105°C is used to cool the entry air and cooling liquid for the second rotor, whose outlet cold air is close to the normal boiling temperature of air.

If experience should show that a linear peripheral velocity of $\sqrt{2}\times 4\times 10^4$ cm/sec. is feasible the energy extraction of the rotor would be doubled as assumed in line 6. Under these circumstances a single step rotor using air and following the CO_2 cycle cooling would give outlet air close to its normal boiling temperature.

When argon is used as the working material, its very small c_p leads to the very large temperature drop of 155°. Argon boils at −185.7°C under 1 atmosphere. Any liquid formed in the rotor will accumulate around the periphery where the extra load may burst the rotor. Still, the argon could be cooled safely near enough to its normal boiling temperature that the compressed air cooled in the exchanger would, on escape through the valve, be 90 percent or so liquid. The vapor part should be used for cooling more compressed air.

19. HIGHLY COMPRESSED GAS IN THE ROTOR

At first glance it looks very advantageous to use in the rotor a gas compressed to well above its critical pressure. The temperature of a gas under such a pressure may be lowered to near freezing conditions without any possibility of separation into two phases, that is, the fluid remains homogeneous. The compressed gas, if cooled slightly below its normal boiling temperature, will be completely liquid on escaping through a valve to atmospheric pressure. Thus the interchanger considered above might be completely avoided and its involved losses not enter the picture. The decreased specific volume of the gas increases greatly the possible mass flow, so increasing the mass capacity of the machine and therefore its efficiency.

On the other hand, there is to be considered the very serious difficulty of transferring a gas under such pressure in and out of the rotor. If the constriction through which the cold liquefied gas expands is placed at the exit from the rotor, and if the gas inlet to the rotor is moved to the

central axial position, the necessary gas-tight moving contacts may be reduced to one. The compressed gas may be passed through several rotors in series on a common shaft, each rotor being supplied between rotors with its necessary separately-cooled liquid. The series arrangement may also be used to cope with the decrease in the temperature drop per rotor owing to the increase in C_p by the compression.

At some point in its cooling, the compressed gas approaches the liquid state—that is, it becomes practically incompressible and changes its temperature relatively little during compression. This takes place markedly only below the critical temperature, but from then on the further cooling in the rotor is likely to be ineffective.

The high pressure will necessitate keeping both fluid and gas in small tubes, preferably one inside the other, and wound as the liquid carrying tubes in Fig. 5, but separating the two tubes at the periphery and returning them to the axis separately. The pressure in the tubes increases the longitudinal tension somewhat but not enough to reduce the maximum rotational speed very materially. It would seem that the possible usefulness of this plan using highly compressed gas in the rotor can only be determined by considerable experimental work.

20. HYDROGEN AND HELIUM LIQUEFACTION

It is interesting to inquire whether such a rotor could serve to reach the very low temperatures of liquid hydrogen and of liquid helium. Lines 8–11 of Table I give some pertinent date on the three possible gases.

It should be noted that the temperatures for this group of gases are given on the Kelvin scale. Neon, line 8, has a low enough c_p (0.246) that it does not need the highest speed of the rotor if used from the boiling temperature of nitrogen (77.2°K) and with nitrogen as the rotor cooling liquid, to escape from the rotor at close to its own boiling temperature 27.3°K. This is of course assuming availability of the very scarce neon.

With liquid neon as cooling liquid and either hydrogen, line 9, or helium, line 10, as working gas, starting at this 27.3°K, the exit gas can be at the boiling temperature of hydrogen (20.4°K).

Starting at this temperature, 20.4°K, with liquid hydrogen as the cooling liquid, helium can escape from the rotor at close to its boiling temperature, 4.21°K.

Too little seems to be known about these liquids to feel safe that none of them will freeze in the rotor at the temperatures and high pressures which well exist there.

In the absence of such misfortunes it thus seems possible to go in a few steps close to the lowest known temperatures.

21. GAS JETS ON THE ROTOR

It may be noted that cooling could also be obtained by discharging the compressed gas at the rotor periphery through jets arranged symmetrically around the rotor and aimed tangentially in the opposite direction to the peripheral velocity, so driving the rotor and cooling the gas. Such jets do not have 100 percent efficiency, and the expansion to the axis appears much to be preferred.

22. ROTOR USE FOR HOUSE HEATING

Kelvin suggested many years ago that the heat delivered by a refrigerating machine be employed for the heating of buildings. When coal is burned under the best conditions in a modern power plant, the work so obtained if applied in an effective refrigerating machine, will raise over the small temperature step needed for this heating, a much greater quantity of heat than that coming directly from the burning of the coal. Since this rotor cooler appears to be the most efficient refrigerator available, it should be effective for the purpose Kelvin suggests.

For the purpose of heat delivery, the rotor-heater should be arranged somewhat differently from the rotor-cooler. The first part of the gas compression should take place adiabatically until the gas temperature rises to that desired for the heating, and in the second part of the compression the gas should flow among the pipes carrying the liquid to be heated, so this part of the compression would be effectively isothermal. The cold discharge gas from the expansion to the axis needs to be warmed by exposure to the building's environment temperature to complete the cycle. Adjustment of the mass flow of the gas and of the speed of the rotor will serve to control the heating.

I wish to express my thanks to Dr. H. Osterberg, Dr. E. E. Miller, Dr. T. A. Murrell, and Dorr Ralph, whose enthusiastic interest in this problem and active discussion of most phases of it have been of great assistance in working out the details of this solution.

The General Theory of Stresses and Displacements in Layered Soil Systems. III*

D. M. BURMISTER
Columbia University, New York, New York

(Received August 24, 1944)

The theory of stresses and displacements for layered soil systems is extended in this paper to cover the more general case of three layers with full continuity across the interfaces between the layers. The three-layer system gives a closer approximation to the actual soil conditions encountered. Only the settlement equation at the surface of the ground is derived at this time, because it has a more direct application to the practical problems of foundation and airport engineering.

INTRODUCTION

FOR most practical problems of foundation and airport engineering, involving the analysis of stresses and displacements, the three-layer system gives a sufficiently close approximation to the actual conditions encountered, because variations in the properties and in the layering of the soils below depths exceeding about twice the diameter or width of the bearing area have a relatively small influence on the load-settlement phenomena of the layered soil profile, as shown by the shape of the influence curves of Fig. 1, paper No. I.

An airport runway is usually made up of the following elements: (*a*) a pavement of concrete or asphalt, (*b*) a base course of compacted crushed stone or gravel, and (*c*) a natural subgrade or a compacted fill. The primary problem is to construct economically sufficient thickness of pavement and base course to provide adequate support for heavy airplane wheel loads by spreading the pressures widely over a weaker subgrade. In order for the pavement to stand up under the direct action of repeated wheel load applications, the settlement or deflection of the pavement and the stresses must be kept below certain limits determined by experience. In foundation engineering serious problems are encountered, where a soft compressible clay layer is sandwiched at some depth between an upper layer of sand and an underlaying layer of sand or rock. A satisfactory foundation design and installation requires that the settlement of the structure, caused by the consolidation of the clay layer under the building load, be reduced to a minimum and be made as uniform as possible within economic limits. Both of these problems require information on the magnitude of the settlement to be expected and the stresses imposed by the loading. It is well known that the upper sand layer in foundation work, or the pavement in the case of airports, has a very important load spreading effect, which considerably reduces the magnitude and the non-uniformity of settlement. The equation for settlement in a three-layer system provides a useful and important tool for the analysis of such problems.

The assumptions and boundary conditions for layered systems were given in paper No. I of this series. Starting with equations No. 6 of this paper for layer No. 1 and similar sets of equations for layers No. 2 and No. 3, the general equation of settlement at the surface of the ground is derived for the three-layer system with full continuity across the interfaces between the three layers.

1. BOUNDARY AND CONTINUITY CONDITIONS. THREE-LAYER SYSTEM

The boundary and continuity conditions, which must be satisfied for the three-layer system are expressed mathematically in the following equations:

(a) Boundary Conditions at the Surface of the Ground, $Z=-H$

Distribution of surface loading, $\sigma_z=-mJ_0(mr)$.

$$-mJ_0(mr)[A_1m^2e^{-mH}+B_1m^2e^{mH}-C_1m(1-2\mu_1+mH)e^{-mH}+D_1m(1-2\mu_1-mH)e^{mH}]=-mJ_0(mr). \quad (29a)$$

Shearing Stress at the Surface, $\tau_{rz}=0$.

$$mJ_1(mr)[A_1m^2e^{-mH}-B_1m^2e^{mH}+C_1m(2\mu_1-mH)e^{-mH}+D_1m(2\mu_1+mH)e^{mH}]=0. \quad (29b)$$

* Publication assisted by the Ernest Kempton Adams Fund for Physical Research of Columbia University.

(b) Continuity Conditions at the Interface between Layers No. 1 and No. 2, $Z=0$

Normal Stress, $\sigma_{z1}=\sigma_{z2}$.

$$[A_1m+B_1m-C_1(1-2\mu_1)+D_1(1-2\mu_1)]=[A_2m+B_2m-C_2(1-2\mu_2)+D_2(1-2\mu_2)]. \quad (30a)$$

Shearing Stress, $\tau_{rz1}=\tau_{rz2}$.

$$[A_1m-B_1m+C_12\mu_1+D_12\mu_1]=[A_2m-B_2m+C_22\mu_2+D_22\mu_2]. \quad (30b)$$

Vertical Settlement, $w_1=w_2$.

$$[(1+\mu_1)/E_1][A_1m-B_1m-C_12(1-2\mu_1)-D_12(1-2\mu_1)]$$
$$=[(1+\mu_2)/E_2][A_2m-B_2m-C_22(1-2\mu_2)-D_22(1-2\mu_2)]. \quad (30c)$$

Horizontal Displacement, $u_1=u_2$.

$$[(1+\mu_1)/E_1][A_1m+B_1m+C_1-D_1]=[(1+\mu_2)/E_2][A_2m+B_2m+C_2-D_2]. \quad (30d)$$

(c) Continuity Conditions at the Interface between Layers No. 2 and No. 3, $Z=+h$

Normal Stress, $\sigma_{z2}=\sigma_{z3}$.

$$[A_2me^{mh}+B_2me^{-mh}-C_2(1-2\mu_2-mh)e^{mh}+D_2(1-2\mu_2+mh)e^{-mh}]$$
$$=[B_3me^{-mh}+D_3(1-2\mu_3+mh)e^{-mh}]. \quad (31a)$$

Shearing Stress, $\tau_{rz2}=\tau_{rz3}$.

$$[A_2me^{mh}-B_2me^{-mh}+C_2(2\mu_2+mh)e^{mh}+D_2(2\mu_2-mh)e^{-mh}]=[-B_3me^{-mh}+D_3(2\mu_3-mh)e^{-mh}]. \quad (31b)$$

Vertical Settlement, $w_2=w_3$.

$$[(1+\mu_2)/E_2][A_2me^{mh}-B_2me^{-mh}-C_2(2-4\mu_2-mh)e^{mh}-D_2(2-4\mu_2+mh)e^{-mh}]$$
$$=[(1+\mu_3)/E_3][-B_3me^{-mh}-D_3(2-4\mu_3+mh)e^{-mh}]. \quad (31c)$$

Horizontal Displacement, $u_2=u_3$.

$$[(1+\mu_2)/E_2][A_2me^{mh}+B_2me^{-mh}+C_2(1+mh)e^{mh}-D_2(1-mh)e^{-mh}]$$
$$=[(1+\mu_3)/E_3][+B_3me^{-mh}-D_3(1-mh)e^{-mh}]. \quad (31d)$$

At infinite depth stresses and displacements in layer No. 3 must be equal to zero. Therefore the coefficients A_3 and C_3 are equal to zero.

(d) Discontinuities at the Interfaces

There is a discontinuity in the radial stress σ_r across each interface, because with the horizontal displacements equal in equations (30d) and (31d) at the interfaces, the radial stresses σ_r either side of each interface must necessarily be determined by the respective modulii, E of the layers.

2. THREE-LAYER SYSTEM COEFFICIENTS

The coefficients in these equations were evaluated to satisfy the boundary and continuity conditions of the three-layer system.

(a) Interface between Layers No. 2 and No. 3, $Z=+h$

The continuity conditions at this interface are satisfied by solving Eqs. (31).

$$2A_2m=2B_2mN(1-4\mu_2-2mh)e^{-2mh}-D_2Le^{-2mh}+D_2N(1-4\mu_2-2mh)(1-4\mu_2+2mh)e^{-2mh}. \quad (32a)$$

$$C_2=2B_2mNe^{-2mh}+D_2N(1-4\mu_2+2mh)e^{-2mh}, \tag{32b}$$

where the strength coefficients for the interface are as follows: E being the modulus and μ being Poisson's ratio.

$$N=\left[\frac{1-n}{1+(3-4\mu_2)n}\right]. \quad L=\left[\frac{(3-4\mu_3)-(3-4\mu_2)n}{(3-4\mu_3)+n}\right]. \quad n=\left[\frac{E_3}{E_2}\times\frac{1+\mu_2}{1+\mu_3}\right]. \tag{32c}$$

(b) Interface between Layers No. 1 and No. 2, $Z=0$

The continuity conditions for this interface are satisfied by solving Eqs. (30) simultaneously with the continuity equations (32) for the interface between layers No. 2 and No. 3 at $z=+h$.

$$\left[2A_1mKN2mhe^{-2mh}+2B_1mK+2B_1m\left(\frac{1-\mu_2}{1-\mu_1}\right)Ne^{-2mh}+2B_1m\left[\frac{(1-\mu_2)(3-4\mu_1)-(1-\mu_1)}{(1-\mu_1)}\right]KNe^{-2mh}\right.$$
$$-C_1-(1-4\mu_1)KN(1+2mh)e^{-2mh}-C_12KNe^{-2mh}-C_1\left(\frac{\mu_1-\mu_2}{1-\mu_1}\right)[1+(3-4\mu_1)K]Ne^{-2mh}$$
$$+D_1(1-4\mu_1)K+D_12KNe^{-2mh}+D_1(1+2mh)Ne^{-2mh}$$
$$\left.-\frac{(\mu_2+3\mu_1-4\mu_1\mu_2)}{(1-\mu_1)}[1+(3-4\mu_1)K]Ne^{-2mh}\right]=0. \tag{33a}$$

$$\left[2A_1mKLe^{-2mh}-2A_1m(1-4\mu_2-2mh)2mhKNe^{-2mh}+2A_1m\left(\frac{1-\mu_2}{1-\mu_1}\right)\right.$$
$$+2A_1m\left[\frac{(1-\mu_2)(3-4\mu_1)-(1-\mu_1)}{(1-\mu_1)}\right]K-2B_1m\left(\frac{1-\mu_2}{1-\mu_1}\right)(1-4\mu_2-2mh)Ne^{-2mh}$$
$$-2B_1m(1-4\mu_2)K-2B_2m\left[\frac{(1-\mu_2)(3-4\mu_1)-(1-\mu_1)}{(1-\mu_1)}\right](1-4\mu_2-2mh)KNe^{-2mh}$$
$$-C_14\mu_2-C_1(1-4\mu_1)KLe^{-2mh}+C_1(1-4\mu_1)(1+2mh)(1-4\mu_2-2mh)KMe^{-2mh}$$
$$+C_1\frac{(\mu_2+3\mu_1-4\mu_1\mu_2)}{(1-\mu_1)}+C_1\left[\frac{(\mu_2+3\mu_1-4\mu_1\mu_2)(3-4\mu_1)-2(1-\mu_1)}{(1-\mu_1)}\right]K$$
$$+C_1\frac{(\mu_1-\mu_2)}{(1-\mu_1)}Ne^{-2mh}+C_1\left[\frac{2(1-\mu_1)+(\mu_1-\mu_2)(3-4\mu_1)}{(1-\mu_1)}\right]KNe^{-2mh}$$
$$+D_14\mu_2(1-4\mu_1)K+D_1Le^{-2mh}-D_1(1+2mh)(1-4\mu_2-2mh)Ne^{-2mh}$$
$$+D_1\frac{(\mu_2+3\mu_1-4\mu_1\mu_2)}{(1-\mu_1)}(1-4\mu_2-2mh)Ne^{-2mh}+D_1\left[\frac{2(1-\mu_1)+(\mu_1-\mu_2)(3-4\mu_1)}{(1-\mu_1)}\right]K$$
$$\left.+D_1\frac{(\mu_1-\mu_2)}{(1-\mu_1)}+D_1\left[\frac{(\mu_2+3\mu_1-4\mu_1\mu_2)(3-4\mu_1)-2(1-\mu_1)}{(1-\mu_1)}\right](1-4\mu_2-2mh)KNe^{-2mh}\right]=0, \tag{33b}$$

where the strength coefficients for layers No. 1 and No. 2 are:

$$K=\left[\frac{1-k}{1+(3-4\mu_1)k}\right], \quad J=\left[\frac{(3-4\mu_2)-(3-4\mu_1)k}{(3-4\mu_2)+k}\right], \quad k=\left[\frac{E_2}{E_1}\times\frac{1+\mu_1}{1+\mu_2}\right]. \tag{33c}$$

(c) Surface of Ground, Layer No. 1, $Z=-H$

The boundary conditions of Eqs. (29) at the surface of the ground are solved, giving the coefficients A_1 and B_1.

$$2A_1m^2=[e^{mH}+C_1m(1-4\mu_1+2mH)-D_1me^{2mH}]; \tag{34a}$$

$$2B_1m^2=[e^{-mH}+C_1me^{-2mH}-D_1m(1-4\mu_1-2mH)]. \tag{34b}$$

Substituting these boundary conditions into the stress and displacement Eqs. (6) of paper No. I, the following equations are obtained for layer No. 1 for settlement and stresses, in terms of C_1 and D_1 only.

Settlement equation at surface, $Z=-H$.

$$w=+J_0(mr)\frac{(1-\mu_1^2)}{E_1}[C_1me^{-mH}+D_1me^{mH}]. \tag{35a}$$

Normal stress equation at interface between layers No. 1 and No. 2, $Z=0$.

$$\sigma_z=-mJ_0(mr)\tfrac{1}{2}[e^{mH}-C_1m(1-2mH)+C_1me^{-2mH}+D_1m(1+2mH)-D_1me^{2mH}+e^{-mH}]. \tag{35b}$$

Shearing stress equation at interface between layers No. 1 and No. 2, $Z=0$.

$$\tau_{rz}=mJ_1(mr)\tfrac{1}{2}[e^{mH}+C_1m(1+2mH)-C_1me^{-2mH}+D_1m(1-2mH)-D_1me^{2mH}-e^{-mH}]. \tag{35c}$$

Similar sets of equations may be obtained for the stresses and displacements at the interface between layers No. 2 and No. 3.

(d) Three-Layer System Coefficients

Solving Eqs. (33) and (34) the coefficients C_1 and D_1 are obtained, which satisfy all of the boundary and continuity conditions of the three-layer system.

$$C_1m=\frac{-\left(\frac{1-K}{1-J}\right)}{\Delta}\left\{\begin{aligned}&+(1+2mH)Ke^{mH}-JKe^{-mH}+(1+2mH)KLNe^{mH}e^{-4mh}\\&+\left[(1+2mH)\left(\frac{1-J}{1-K}\right)K^2L+4m^2h^2(1+2mH)\left(\frac{1-J}{1-K}\right)K^2N+2mhN\right.\\&\qquad\left.+(1+2mH)\left(\frac{1-K}{1-J}\right)N-2mhJKN\right]e^{mH}e^{-2mh}\\&-\left[\left(\frac{1-K}{1-J}\right)JN+\left(\frac{1-J}{1-K}\right)KL+4m^2h^2\left(\frac{1-J}{1-K}\right)KN\right]e^{-mH}e^{-2mh}\\&-LNe^{-mH}e^{-4mh}\end{aligned}\right\}, \tag{36c}$$

$$D_1m=\frac{-\left(\frac{1-K}{1-J}\right)}{\Delta}\left\{\begin{aligned}&+e^{mH}-(1-2mH)Ke^{-mH}-(1-2mH)KLNe^{-mH}e^{-4mh}\\&+\left[\left(\frac{1-K}{1-J}\right)JN+\left(\frac{1-J}{1-K}\right)KL+4m^2h^2\left(\frac{1-J}{1-K}\right)KN\right]e^{mH}e^{-2mh}\\&-\left[(1-2mH)\left(\frac{1-K}{1-J}\right)N+(1-2mH)\left(\frac{1-J}{1-K}\right)K^2L-2mhN\right.\\&\qquad\left.+(1-2mH)4m^2h^2\left(\frac{1-J}{1-K}\right)K^2N+2mhJKN\right]e^{-mH}e^{-2mh}\\&+JKLNe^{mH}e^{-4mh}\end{aligned}\right\}, \tag{36d}$$

$$\Delta=-\left(\frac{1-K}{1-J}\right)\begin{bmatrix}+e^{2mH}-[J+(1+4m^2H^2)K]+JKe^{-2mH}\\ -\left[\left(\frac{1-K}{1-J}\right)N+\left(\frac{1-J}{1-K}\right)L+\left(\frac{1-J}{1-K}\right)4m^2h^2N\right]e^{-2mh}+LNe^{-2mH}e^{-4mh}\\ -\left[(1+4m^2H^2)\left(\frac{1-J}{1-K}\right)K^2L+4m^2h^2(1+4m^2H^2)\left(\frac{1-J}{1-K}\right)K^2N\right.\\ \left.+\left(\frac{1-K}{1-J}\right)J^2N+8mHmh(1-JK)N+4m^2H^2\left(\frac{1-K}{1-J}\right)N\right]e^{-2mh}\\ +\left[JN+\left(\frac{1-J}{1-K}\right)KL+4m^2h^2\left(\frac{1-J}{1-K}\right)KN\right][e^{2mH}e^{-2mh}+e^{-2mH}e^{-2mh}]\\ -[(1+4m^2H^2)KLN+JLN]\cdot e^{-4mh}+JKLNe^{2mH}e^{-4mh}\end{bmatrix}, \quad (36e)$$

3. THREE-LAYER SETTLEMENT EQUATION AT THE SURFACE OF GROUND

The settlement equation at the surface of the ground, for a surface loading with a distribution, $\sigma_z=-mJ_0(mr)$ is derived by substituting the coefficients C_1 and D_1 of Eqs. (36) into Eq. (35a). It is to be noted that the numerator and denominator fall into a rather remarkable pattern.

$$w=+J_0(mr)\left[\frac{1-\mu_1^2}{E_1}\right]\left[\frac{\text{Numerator}}{\text{Denominator}}\right] \quad (37)$$

$$\text{Numerator}\begin{bmatrix}1+4mHKe^{-2mH}-JKe^{-4mH}+4mhNe^{-2mH}e^{-2mh}-LNe^{-4mH}e^{-4mh}\\ +\left[4mH\left(\frac{1-J}{1-K}\right)K^2L+16mHm^2h^2\left(\frac{1-J}{1-K}\right)K^2N\right.\\ \left.+4mH\left(\frac{1-K}{1-J}\right)N-4mhJKN\right]e^{-2mH}e^{-2mh}\\ +\left[\left(\frac{1-K}{1-J}\right)JN+\left(\frac{1-J}{1-K}\right)KL+4m^2h^2\left(\frac{1-J}{1-K}\right)KN\right][e^{-2mh}-e^{-4mH}e^{-2mh}]\\ +4mHKLNe^{-2mH}e^{-4mh}+JKLNe^{-4mh}.\end{bmatrix},$$

$$\text{Denominator}\begin{bmatrix}1-[J+K+4m^2H^2K]e^{-2mH}+JKe^{-4mH}\\ -\left[\left(\frac{1-K}{1-J}\right)N+\left(\frac{1-J}{1-K}\right)L+4m^2h^2\left(\frac{1-J}{1-K}\right)N\right]e^{-2mH}e^{-2mh}+LNe^{-4mH}e^{-4mh}\\ -\left[(1+4m^2H^2)\left(\frac{1-J}{1-K}\right)K^2L+4m^2h^2(1+4m^2H^2)\left(\frac{1-J}{1-K}\right)K^2N+\left(\frac{1-K}{1-J}\right)J^2N\right.\\ \left.+8mHmh(1-JK)N+4m^2H^2\left(\frac{1-K}{1-J}\right)N\right]e^{-2mH}e^{-2mh}\\ +\left[\left(\frac{1-K}{1-J}\right)JN+\left(\frac{1-J}{1-K}\right)KL+4m^2h^2\left(\frac{1-J}{1-K}\right)KN\right][e^{-2mh}+e^{-4mH}e^{-2mh}]\\ -[(1+4m^2H^2)KLN+JLN]e^{-2mH}e^{-4mh}+JKLNe^{-4mh}\end{bmatrix}.$$

The strength coefficients N and L involving layers No. 2 and No. 3 are given by Eqs. (32c) and the strength coefficients, K and J involving layers No. 1 and No. 2 are given by Eq. (33c). The thickness of layer No. 1 is H and of layer No. 2 is h.

The following checks were made on this settlement equation to verify its correctness of form. (*a*) If the thickness of layer No. 1, H equals zero and the strength coefficients K and J are equal to zero (since layer No. 1 does not exist, $E_2=E_1$ and $\mu_2=\mu_1$), the settlement equation reduces to the form of the two-layer Eq. (11) of paper No. I.

$$w=J_0(mr)\frac{1-\mu_2^2}{E_2}\left[\frac{1+4mhNe^{-2mh}-LNe^{-4mh}}{1-(N+L+4m^2h^2N)e^{-2mh}+LNe^{-4mh}}\right]. \tag{38a}$$

(*b*) If the thickness of layer No. 2 becomes infinite and the strength coefficients N and L are equal to zero (since layer No. 3 does not exist, $E_2=E_3$ and $\mu_2=\mu_3$), the settlement equation again reduces to the form of the two-layer equation.

$$w=J_0(mr)\frac{1-\mu_1^2}{E_1}\left[\frac{1+4mHKe^{-2mH}-JKe^{-4mH}}{1-(J+K+4m^2H^2K)e^{-2mH}+JKe^{-4mH}}\right]. \tag{38b}$$

(*c*) Finally, the most significant test, which involves all but 4 terms each of the numerator and denominator (*mh*-terms), shows that, if the thickness, h of layer No. 2 equals zero, the settlement equation again reduces to the two-layer equation for layers No. 1 and No. 3 only. Making $h=0$ and collecting terms and simplifying, Eq. (37) becomes:

$$w=J_0(mr)\frac{1-\mu_1^2}{E_1}\left[\frac{\text{Numerator}}{\text{Denominator}}\right]. \tag{38c}$$

$$\left\{\begin{array}{l}\dfrac{1+4mH\left[\overbrace{\dfrac{K-JK-KN+N}{1-J+JN-JKN}}^{K'}\right]e^{-2mH}-\left[\overbrace{\dfrac{K-JK-KN+N}{1-J+JN-JKN}}^{K'}\right]\left[\overbrace{\dfrac{J-JK-JL+L}{1-K+KL-JKL}}^{J'}\right]e^{-4mH}}{1-\left[\left[\overbrace{\dfrac{K-JK-KN+N}{1-J+JN-JKN}}^{K'}\right]+\left[\overbrace{\dfrac{J-JK-JL+L}{1-K+KL-JKL}}^{J'}\right]+4m^2H^2\left[\overbrace{\dfrac{K-JK-KN+N}{1-J+JN-JKN}}^{K'}\right]\right]e^{-2mH}} \\ \qquad\qquad +\left[\overbrace{\dfrac{K-JK-KN+N}{1-J+JN-JKN}}^{K'}\right]\left[\overbrace{\dfrac{J-JK-JL+L}{1-K+KL-JKL}}^{J'}\right]e^{-4mH}\end{array}\right\}.$$

By substituting the values of the strength coefficients of Eqs. (32c) and (33c) it may be readily shown that the above strength coefficients K' and J' involving layers No. 1 and No. 3 for the two-layer system reduce to the forms below.

$$K'=\left[\frac{1-kn}{1+(3-4\mu_1)kn}\right],\quad J'=\left[\frac{(3-4\mu_3)-(3-4\mu_1)kn}{(3-4\mu_3)+kn}\right], \tag{38d}$$

where

$$kn=\left[\frac{E_2}{E_1}\frac{1+\mu_1}{1+\mu_2}\right]\times\left[\frac{E_3}{E_2}\frac{1+\mu_2}{1+\mu_3}\right]=\left[\frac{E_3}{E_1}\frac{1+\mu_1}{1+\mu_3}\right].$$

The numerical evaluation of the settlement Eq. (37) for the three-layer system for practical use will require a series of diagrams similar to Fig. 1 of paper No. I, covering a suitable range of values for each of the basic parameters, namely the strength coefficients k and n for the three layers, and the thickness H of layer No. 1, and h of layer No. 2, expressed as the ratio, $a=h/H$. For most practical problems in foundation engineering, when dealing with the consolidation of deeply buried

clay layers, it can be assumed without serious error that a rock surface exists at the base of layer No. 2. With $E_3 = \infty$ for rock, the strength coefficients N and L both become equal to minus one (-1), which considerably simplifies the settlement equation for numerical evaluation. The equations for normal and shearing stresses at the interface between layers No. 1 and No. 2 may be obtained by substituting the coefficients C_1 and D_1 of Eqs. (36) into Eqs. (35b) and (35c), and into a similar set of equations for the interface between layers No. 2 and No. 3.

Stability of Low Pressure Mercury Arcs as a Function of Current

PAUL COPELAND, *Department of Physics, Illinois Institute of Technology, Chicago, Illinois*

AND

W. H. SPARING, *Bureau of Ships, Navy Department, Washington, D. C.*

(Received December 7, 1944)

The persistence of an arc in an experimental tube with a pool type cathode has been studied. The mean life under carefully controlled operating conditions is determined by statistical analysis of a hundred or more observed lives and is taken as a measure of the stability. The dependence of mean life upon both the ambient temperature of the cathode pool and the current is determined. The arc is found to be most stable at an optimum ambient temperature. In the first observations the cathode spot was free; later observations were made with the cathode spot anchored in contact with a tungsten film. In both cases the results indicate that the mean life rises exponentially with the arc current in the ranges used. If I represents the arc current and L represents its average duration, the results suggest a relationship of the form

$$L = F(p, x, y, z, \cdots) \exp(kI),$$

where F stands for some functional relationship depending on the mercury vapor pressure p calculated from the ambient temperature, and upon other parameters such as x, y, and z, at present undetermined. For the proportionality constant k, the data give (2.46 ± 0.06) ampere^{-1} when the cathode spot is free and (19.92 ± 0.47) ampere^{-1} when the cathode spot is anchored. $F(p, x, y, z, \cdots)$ appears to be smaller with the cathode spot anchored than with it free, but the probable error in the function is relatively large.

THE general criterion for stable operation of an arc was set forth by Kaufmann[1] and developed further by Dallenbach[2] and Ives.[3] As the current through the arc increases, the potential difference across it falls; so that the arc itself is characterized by a negative resistance. Kaufmann stated that for the arc to operate stably the ordinary resistance in series with it must be sufficient to make the total resistance positive.

In Fig. 1, the dotted curve shows the characteristics of an arc. Here the abscissas represent current, and the ordinates represent potential difference. Slopes are proportional to resistance. The downward trend of the V–I plot for the arc represents the negative resistance. For low values of current the negative resistance is high, but as the current increases the negative resistance decreases. A possible characteristic for the external impedance is represented by the fine solid line. The resistance may change as a function of the current, and in general the external resistance should not be represented by a straight line. The sum of the potential differences across the arc and the external resistance is represented by the heavy solid curve having a broad minimum. According to Kirchhoff's loop rule, the potential represented by the heavy curve would equal the

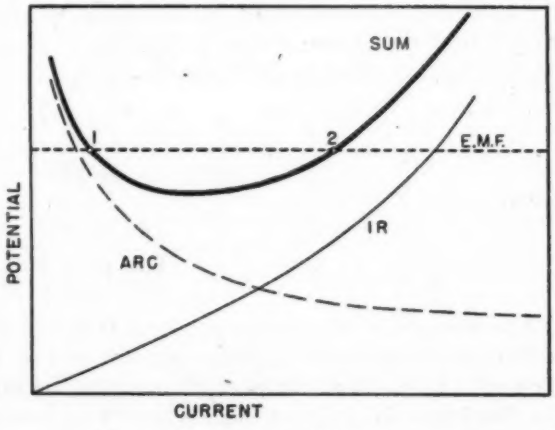

FIG. 1. Operating conditions for an arc.

[1] W. Kaufmann, Ann. d. Physik [4] **2**, 158 (1900).
[2] W. Dallenbach, Physik. Zeits. **27**, 101 (1926).
[3] H. E. Ives, J. Frank. Inst. **198**, 437 (1924).

applied electromotive force. In the usual arc circuit an effort is made to maintain the electromotive force constant, and it would be represented by a horizontal line on the graph. If the electromotive force is not high enough to intersect the curve representing the sum of the potential differences, it is not sufficient to operate the arc paired with this resistor. Although an electromotive force great enough to operate the arc will cut the curve in two places, only one of these would provide a stable operating point according to Kaufmann's criterion. At a point such as 1 the total resistance is negative, and a small increase in the current will give rise to circuit conditions causing the arc to seek point 2 as its stable operating condition, because at this point the total resistance is positive.

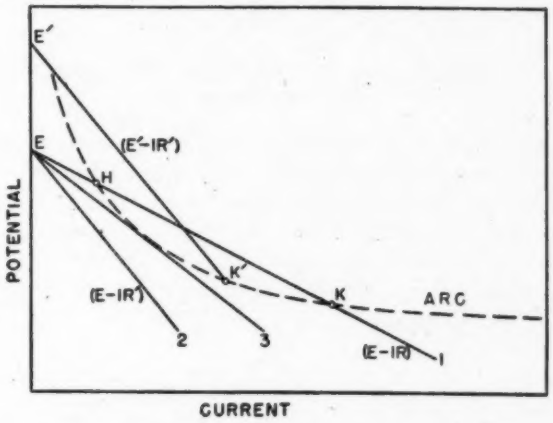

FIG. 2. Conditions in circuit containing an arc.

Representation of conditions for arc stability is sometimes changed as a matter of convenience. In Fig. 2, the dotted curve represents the arc characteristic, but in this graph the characteristic of the electromotive force and the added impedance combined is shown by plotting $(E-RI)$ as a function of I, where E represents the electromotive force in the circuit, and RI is the potential drop across the resistor. Kirchhoff's loop rule is satisfied wherever the $(E-RI)$ line intersects the arc curve, as at points H and K. Kaufmann's criterion restricts the operation of the arc to the lower point K. If the resistance in series with the arc is too large, as shown by line 2, the $(E-RI)$ line does not cut the arc curve, and the conditions for the operation of the arc are not satisfied. Of course, by increasing the value of E coupled with the high resistance the arc might be made to operate at a lower current than it otherwise would. This is shown by the line

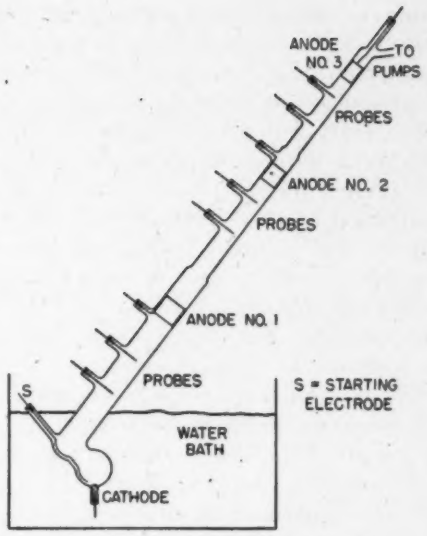

FIG. 3. Experimental tube.

marked $(E'-R'I)$. Even with the lower electromotive force if the resistance is quite low, as represented in the figure by line 1, the arc will operate with a high degree of stability at the point K. The line marked 3 divides the conditions for operation from those for nonoperation. From physical considerations it would seem surprising if this transition from stability to instability were as sharp and definite as this discussion would appear to indicate. It seems more likely that the arc should become less and less stable as, by gradually increasing the resistance, the conditions shown by line 3 are approached. The experiments reported in this paper substantiate this view, and the stability of an arc has been investigated quantitatively under various carefully controlled operating conditions.

EXPERIMENTAL ARRANGEMENT

The mercury arc used in these studies, which is shown schematically in Fig. 3, was used for other studies also, and its design is somewhat more complicated than would be essential for the experiments to be discussed. Basically the tube consists of a 250-cc Pyrex glass flask, containing the cathode pool, sealed onto a section of straight tubing sufficient for a long positive column in the discharge. Along the length of the straight tubing there are a number of electrodes any one of which may be used for the anode. There is a bend between the cathode bulb and the positive column, and for the purpose of maintaining the vapor pressure of mercury constant during the

operation of the arc, the entire cathode bulb and a portion of the straight tube beyond the bend are immersed in a water bath of large capacity. For convenience in starting the arc, a probe of tungsten wire, sealed through the bend, extends to within a few millimeters of the mercury pool surface. When the arc is to be started, the negative terminal of the electromotive force is connected to the cathode pool, and the positive terminal of the electromotive force is connected through a suitable resistance to one of the anodes. The application of 25,000 volts to the starting probe initiates a cathode spot on the pool of mercury. If conditions are correct, the discharge is transferred to the main electrodes, and the arc continues after the potential has been removed from the starting probe.

After the experimental tube was assembled, it was connected to a vacuum line consisting of a three stage mercury diffusion pump backed by a rotary mechanical pump. Mercury from a side tube was distilled into the cathode pool to such a level that the area of the free surface was 23 cm^2.

An effort was made to keep circuit conditions constant during a set of measurements for determining stability. The pressure of residual air, as read on a McLeod gauge, was maintained at 10^{-6} mm Hg or less. The electromotive force used for maintaining the arc was supplied from direct current mains which measured between 105 and 106 volts with the arc in operation. The impedance in series with the arc consisted of a number of wire wound variable rheostats rated for ample power dissipation, so that the heating in the course of the tests did not result in a change of current great enough to be observable on the meters. The water bath, in which the entire cathode end of the tube was immersed, was circulated constantly by a motor driven stirrer, and the temperature of the bath as read by a mercury thermometer was not allowed to vary more than 0.2°C.

In spite of these efforts to maintain constancy for the operation of the arc, conditions are far from static. Ordinarily a brilliant spot dances around on the surface of the cathode pool in a most erratic fashion, and as a consequence there is some mechanical agitation of the surface. If either the current through the arc or the voltage across it is examined with the aid of a cathode ray oscilloscope, continual random fluctuations are observed. These fluctuations are not large. They are of rather short duration. They are entirely irregular, and they are continually occurring.

In such an arc the division between stability and instability is not as sharp as one would expect from the Kaufmann criterion. It appears that the arc has a finite probability of going out under any operating conditions. This probability changes gradually in response to circuit factors, and it changes in the sense which is suggested by the Kaufmann criterion and the shape of the arc characteristic. If the arc is started, it runs for a time before it goes out. If it is started again under the same circumstances, it is likely to run for a different time and go out again. As a result of a large number of observations, the average life may be determined. Statistical analysis of the observed lives confirms the hypothesis that there is a finite probability for the extinction of the arc whenever it is in operation, and the data may be treated in much the same way as those for radioactive decay.

CONSIDERATIONS UNDERLYING THE ANALYSIS OF THE DATA

If a large number of identical arcs were to be operated simultaneously, each would have the same probability λ of going out during each second of its life. The number of extinctions during a short time interval dt would be proportional to the product of dt and N, the number of arcs operating at the time. Thus

$$dN = -\lambda N dt.$$

Integration gives

$$N = N_0 \exp(-\lambda t), \qquad (1)$$

where N_0 is the number of arcs operating at the time t is zero. For convenience in the representation of the results, the natural logarithm of each side of Eq. (1) is taken, which gives

$$\ln N - \ln N_0 = -\lambda t. \qquad (2)$$

Hence so long as the number of arcs is large, the logarithm of the number remaining lighted is a linear function of the time, and the slope λ of the semi-logarithmic plot is easily shown to be the reciprocal of the average life.

Of course, it makes no difference whether the experiment is made with a great number of identical arcs or whether the test is repeated a large number of times with the same arc. In the experiments to be reported many tests were made with the experimental tube which has been described. The data obtained under fixed operating conditions are analyzed by plotting the logarithm of N the number of times that the arc

remained in operation for more than t seconds as a function of t. The average life, which is taken as a measure of the stability under the conditions of operation, is found from the reciprocal of the slope in such a plot.

If instead of a very large number of observations only a finite number is used, the underlying analysis is the same, but if the details were preserved, the time of extinction for any test would correspond to a discrete step in the semi-logarithmic plot. This is not a fundamental difficulty, because it can be circumvented by drawing the straight line which best represents the experimental data. Statistical fluctuations due to the finite number of tests, however, limit the accuracy to be expected. R. Peierls[4] has discussed the statistical errors in counting experiments and has shown that the best approximation to the mean life T of a population is the arithmetic mean of the observed individual lives, and that the relative mean error in the average is given by

$$\overline{\delta T^2}/T^2 = 1/N, \qquad (3)$$

where N is the number of counts. Application of the usual relationship between the mean error and the probable error results in a value of $0.6745/N^{\frac{1}{2}}$ for the probable relative error. Less than 100 trials would hardly be satisfactory for determination of the average life, but something over 100 trials should result in a probable error of about six percent. Since the accuracy increases only as the square root of the number of tests, the determination of the average life with an accuracy of an order of magnitude higher than this figure would involve labor unwarranted at present.

Observations are made by establishing a set of desired operating conditions for the arc which are maintained constant throughout a complete set of tests. The arc is initiated by the application of potential to the starting probe, and as soon as the discharge has transferred to the main electrodes, the timing is begun. When the arc goes out, the timing is stopped, and the observation is recorded. This process is repeated under the same conditions for at least a hundred trials. The device used for timing the longer lives was a stop watch. For the shorter lives a Cenco impulse counter operated from the 60-cycle mains was used; so that a second was divided into 120 equal-time intervals. The timing devices were started and stopped manually, and the reaction time of the observer would naturally influence the results, but errors due to this cause should not be large. Since the slope of the semi-logarithmic plot is used for the estimation of the average life, the addition of equal times to each observation does not have a primary bearing on accuracy. Errors in making measurements of time would limit the accuracy in the average life to the probable error introduced by small variations in the reaction time, and in no case was the accuracy expected sufficient to make this a limiting factor. The probable error in the results is dominated by statistical fluctuations, and on the basis of statistical theory it is estimated directly from the number of trials.

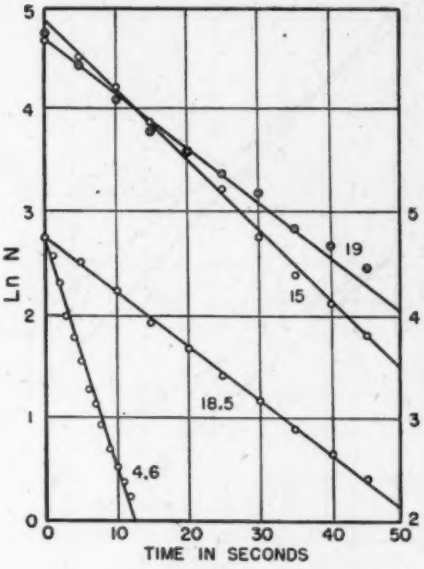

FIG. 4. Life of 3-ampere arc.

DISCUSSION OF RESULTS

Representative results obtained early in these studies are shown in Fig. 4 and Fig. 5. All the data in Fig. 4 were obtained with an arc current of 3.0 amperes, while all the data in Fig. 5 were obtained with 4.0 amperes. In all cases the logarithm of the number of trials in which the arc ran longer than t seconds is plotted as a function of t. The preceding section has shown that except for the effect of statistical fluctuations the experimental data when analyzed in this way should fall along a straight line. The results verify this prediction. The very great increase in the stability of the arc when operated on 4.0 amperes is indicated by the difference in scale on the axis of abscissas, which is almost tenfold. In Fig. 4 and Fig. 5 the scale of ordinates on the left-hand

[4] R. Peierls, Proc. Roy. Soc. **A149**, 467 (1935).

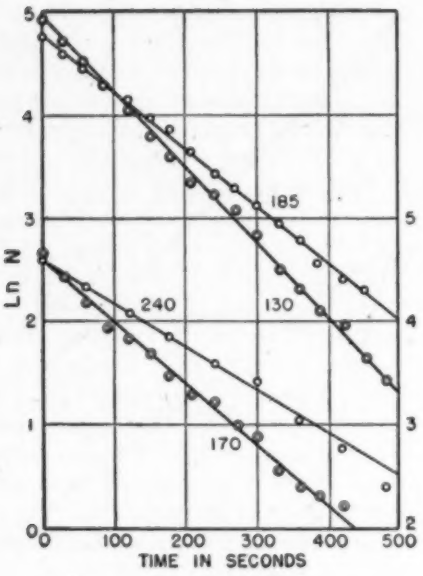

FIG. 5. Life of 4-ampere arc.

margin applies to the two upper curves, and the scale of ordinates on the right-hand margin applies to the two lower lines. The average lives in seconds, as determined from the reciprocals of slope, are shown by the numerals used to identify the lines.

With 3.0 amperes of arc current and the bath surrounding the cathode pool maintained at a temperature corresponding to a vapor pressure of 0.0012 mm Hg, the arc has an average life of only 4.6 seconds. When the temperature of the bath is raised to allow for a vapor pressure of 0.00184 mm, the arc life increases to 15 seconds. When the indicated pressure is 0.00278 mm the life is 19 seconds. When the pressure is 0.00414 mm, the life is 21 seconds, and when the pressure is 0.00608 mm, the average life drops to a value of 18.5 seconds.

The probable error in the slope, as indicated by the spread of the experimental points, would not be large. The line giving the 18.5-second average life fits the experimental points with greater precision than would be expected from slightly more than 100 observations. On the other hand, statistical fluctuations are quite evident in the scattering of the experimental points about the 15- and 19-second lines. The scattering of experimental points about the 4.6-second line would be just as evident as in the other cases if the scale of abscissas were expanded. The slope of the 18.5-second line would appear to be determined by the experimental points with a probable relative error of only 3.8 percent. The probable relative error expected on the basis of statistical theory would be 6.2 percent for a sample of this size. On the other hand, the line giving a reciprocal slope of 19 seconds has a spread of points indicating a probable error of 7.6 percent, whereas the probable error predicted from the size of the sample is 6.5 percent. There is little doubt that the reciprocal slopes of all other lines both in Fig. 4 and Fig. 5 are determined with a relative error which is very close to that calculated directly from the number of observations, and the result given by statistical theory will be used for the estimation of probable error.

A summary of results is contained in Table I. There can be little doubt that at a given current, there is an optimum temperature for the operation of the cathode pool. Figure 6 shows the average life of the three-ampere arc as a function of the vapor pressure calculated from the temperature of the water bath surrounding the cathode pool. The initial increase in the average life as a function of vapor pressure is so pronounced as to make the trend of the points certain. The probable relative errors for the points are of the order of 6 percent, and the observed decrease is 12 percent. Hence the decrease of the average life beyond the maximum would be considered significant in any case, but it is further supported by the regularity of the trend for the entire set.

The average life increases very rapidly as a function of the current. The results for two different ambient temperatures are shown in Fig. 7. Here the average life is plotted loga-

TABLE I. Stability data.

Arc current (amperes)	Vapor pressure of mercury corresponding to ambient temperature (microns Hg)	Average life (seconds)	Probable relative error (percent)
2.5	1.2	1.5	6.7
2.5	6.08	5.9	6.4
3.0	1.2	4.6	6.1
3.0	1.84	15.0	6.6
3.0	2.78	19.0	6.4
3.0	4.14	21.0	6.7
3.0	6.08	18.5	6.2
3.5	1.2	15.0	6.3
4.0	1.2	130.0	5.6
4.0	1.84	170.0	6.6
4.0	2.78	185.0	6.2
4.0	6.08	240.0	6.7
0.40	1.2	2.7	6.7
0.45	1.2	5.2	6.7
0.50	1.2	21.0	6.4
0.55	1.2	48.0	6.7
0.60	1.2	145.0	6.7

rithmically on the vertical scale, and the arc current in amperes is plotted along the horizontal axis. Six experimental points support the validity of the lines drawn in Fig. 7. The seventh point is so far in error that the rules of statistics indicate that it should be ignored. The experimental average life of 130 seconds, having a calculated probable error of 5.6 percent, would need to be divided by a factor of more than two if it were to be brought down onto the line established by the other data. Such a variation cannot be explained by statistical fluctuations; it must be due to an undetermined cause.

If the point off the lower line is ignored, the remaining data may be represented by a relationship of the form

$$L = F(p, x_0, y_0, z_0) \exp(kI),$$

where L stands for the average life, I stands for the arc current, and p is the mercury vapor pressure corresponding to the temperature of the bath surrounding the cathode. Other conditions, specified by the parameters x, y and z, may influence the average life, but in this experiment an effort was made to eliminate any variations from these causes by maintaining experimental conditions constant. The data give: (2.46 ± 0.06) ampere^{-1} for k, while $F(p, x_0, y_0, z_0)$ is 0.011 second for $p = 0.00608$ mm Hg, and 0.0028 second for $p = 0.0012$ mm Hg.

A circumstance which radically altered the operating characteristics occurred when an arc

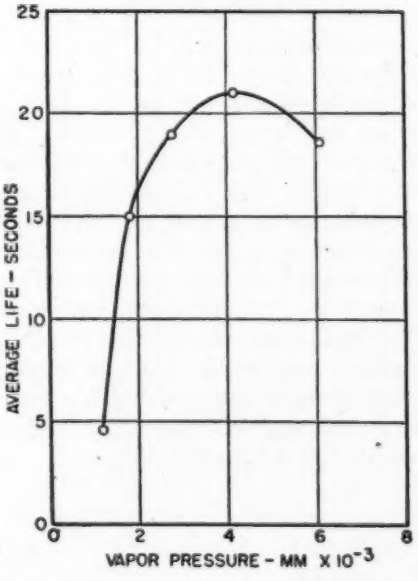

FIG. 6. Average life of 3-ampere arc as a function of mercury vapor pressure.

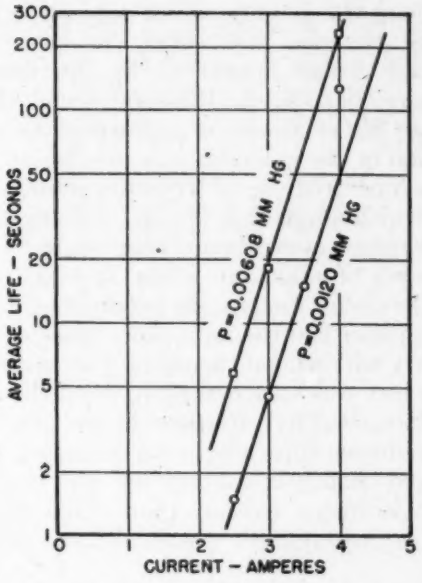

FIG. 7. Average life as a function of arc current.

was struck to the tungsten electrode or probe in the main tube nearest the cathode pool. The power generated at the probe was sufficient to vaporize the tungsten, which was then deposited in a thin film over the inner glass wall of the arc tube including the line of contact between the cathode pool and the glass. When this had happened, the cathode spot attached itself to a definite point on what appeared to be the line of contact between the mercury and the tungsten film. This so greatly increased the stability of the arc that it would operate on a very small fraction of the current previously required. The instability of the arc became apparent only when the current was reduced to a fraction of an ampere.

Life data for the arc operating with an anchored cathode spot are shown in Fig. 8. In this figure the scale of abscissas in the upper margin applies to the dashed curve, and the scale of abscissas in the lower margin to the solid curves. As before, when the logarithm of the number of times that the arc ran longer than t seconds is plotted as a function of t, the experimental points fall along a straight line, and the spread of the points is of correct magnitude to be attributed to statistical fluctuations. These data are summarized in the latter part of Table I, and, as shown in Fig. 9, the average life increases exponentially with the arc current over the range of currents investigated. In this case the data give: (19.92 ± 0.47) for k and about 9.6×10^{-4} for $F(p, x_0, y_0, z_0)$, but the probable relative error in the latter is about 40 percent.

Among the conditions not subject to definite control the one most likely to influence the accuracy would appear to be distributed inductance. Mr. F. A. Ransom[5] found that the average life of an arc is approximately a linear function of the inductance in the circuit. An arc which operated in a virtually non-inductive circuit with an average life of 1.2 seconds had its life increased approximately one second for each millihenry of inductance added in series with the arc. The circuit used for the experiments reported in this paper had the inductance associated with ordinary wire wound rheostats. Furthermore the inductance was varied slightly when the current was changed. The variations in the average life expected from this cause would be small, and the observed change in average life was very large. The experiments indicate that within the limits of experimental error dominated by statistical

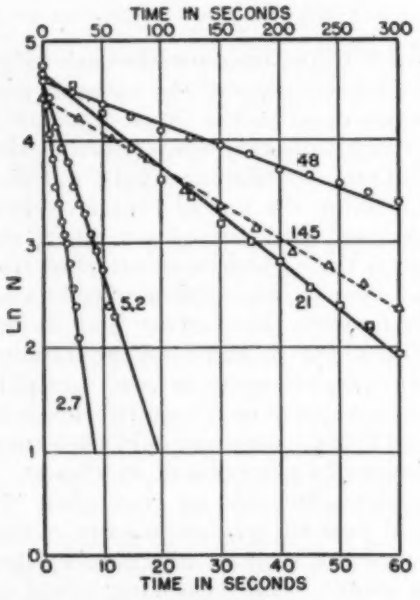

FIG. 8. Arc life with cathode spot anchored.

considerations the average life varies exponentially as a function of the current.

The introductory discussion of Kaufmann's criterion presented reasons for believing that the

[5] F. A. Ransom, unpublished Master's Thesis, Department of Physics, Illinois Institute of Technology, 1941.

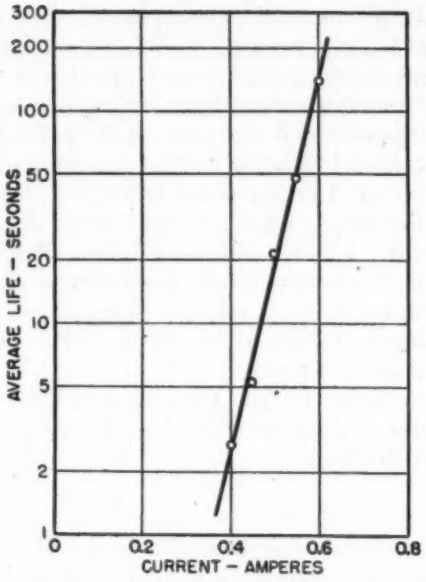

FIG. 9. Relationship between current and average life of arc with cathode spot anchored.

average life of an arc should depend upon the electromotive force in the circuit. In these experiments the electromotive force was so nearly constant that variations from this cause would be negligible. The method of investigation presented here could be used for quantitative studies of the dependence of arc stability upon electromotive force and upon a variety of other operating conditions.

CONCLUSIONS

The variation of arc stability with the temperature of the bath surrounding the cathode pool is believed to be significant, and to indicate that there is an optimum vapor pressure, depending upon the current, at which the maximum stability is attained. The average life shows a continuous variation with the arc current, and the evidence obtained in these experiments indicates that the average life is an exponential function of the arc current. There is much evidence to show that the extinction of the arc depends upon uncontrolled circumstances in the neighborhood of the cathode spot, and there was a spectacular increase in arc stability when the cathode spot was anchored at a tungsten film.

The Validity of the Pole Figure

BEULAH FIELD DECKER
General Electric Company, Schenectady, New York
(Received December 27, 1944)

A [110] pole figure for cold-rolled and annealed silicon steel, constructed from data obtained with an integrating x-ray camera, is compared with a stereographic projection of [110] poles for one hundred individual grains in the same samples. From this comparison, it is concluded that pole figures are accurate enough to determine preferred orientations when the exact percentage of crystals in each orientation is not required.

THE preferred orientation in rolled metal is usually determined by constructing a pole figure. This pole figure is a stereographic projection of the poles of certain lattice planes (in silicon steel the (110) planes), the intensity of any spot on the pole figure being proportional to the density of poles along the corresponding direction in the rolled strip. The data used in constructing the pole figure are obtained from a series of transmission x-ray diffraction patterns taken with an integrating camera, and for each pattern the sample is inclined at a different angle to the x-ray beam.

The validity of a pole figure constructed from such data has been a matter of speculation, and so the author wishes to report some results which show that such a pole figure represents the actual distribution of poles as accurately as could be desired.

The sample used for the present work is a strip of cold-rolled and annealed silicon steel. The grain size is small enough to enable the sample to be used with the integrating camera, but also large enough so that single crystal back reflection photographs of separate grains could be taken.

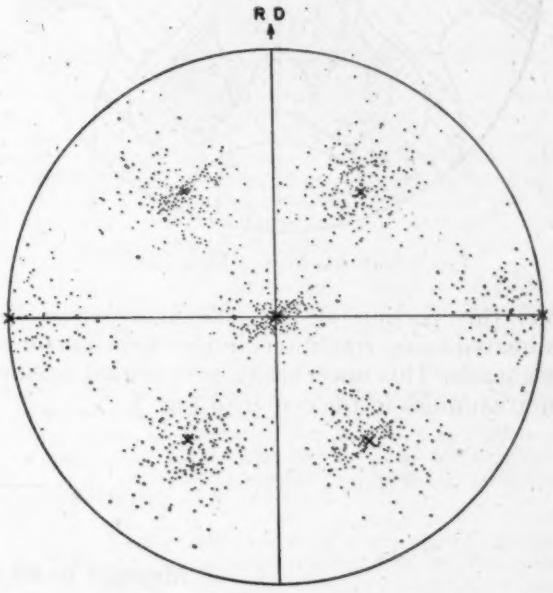

FIG. 2.

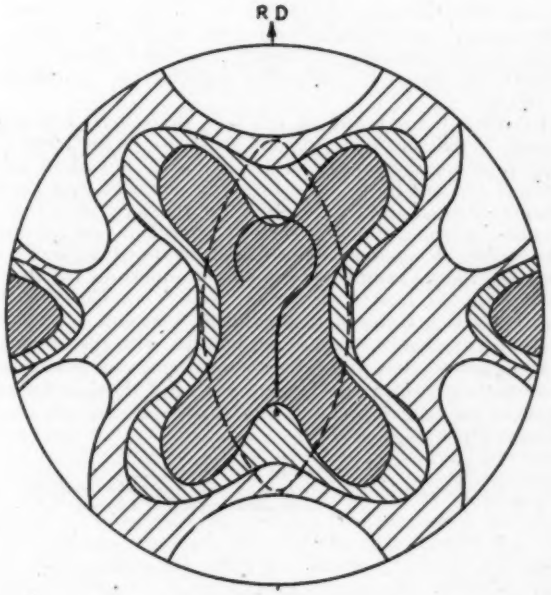

FIG. 1.

Figure 1 is the [110] pole figure of the sample constructed from data obtained with an integrating x-ray camera. A high degree of preferred orientation is shown, most of the crystallites having a (110) plane nearly in the plane of rolling and a [100] direction nearly in the direction of rolling. Data cannot be obtained for the central portion of the pole figure because of the difficulty in obtaining photographs when the angle between the x-ray beam and the plane of the sample becomes small, and also because of the large errors present due to absorption of the x-rays in passing through the specimen.[1] There-

[1] B. F. Decker, Proc. A. S. T. M. **43**, 799 (1943).

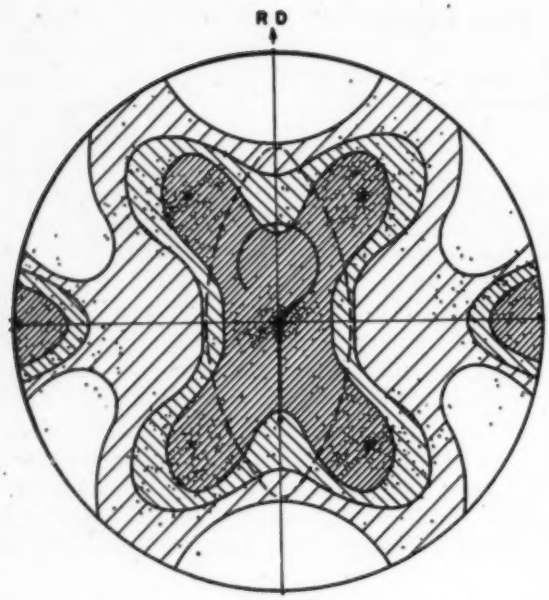

FIG. 3. Superposition of Figs. 1 and 2.

fore, this portion of the pole figure must be estimated using conditions in the outer portions as a guide. This uncertainty is indicated by the question mark in the center of Fig. 1.

After the pole figure of Fig. 1 was obtained, back reflection x-ray photographs were taken of one hundred individual grains chosen at random in the sample. The positions of [110] poles were determined for each of these grains, and a stereographic plot of these poles is shown in Fig. 2. The crosses mark the ideal orientation with a (110) plane in the plane of rolling and [100] direction in the direction of rolling. In order to see more easily the correlation between Figs. 1 and 2, they are shown superimposed in Fig. 3. This shows clearly how nearly alike the two figures are. The only differences are contained in the central region where the pole figure is estimated.

Therefore, it may be concluded that pole figures, constructed from data obtained with an integrating x-ray camera are accurate enough to determine preferred orientations when the exact percentage of crystals in each orientation is not required.

The author wishes to express her appreciation to Mr. Eric T. Asp for the x-ray photographs used in this work, and to Dr. David Harker for helpful criticism of the paper.

A Message to All Interested in Physics

You have probably heard the story of the young mother of the baby that was a year old before the last payment was made to the doctor. Her exclamation was, "Now we own the baby." The headquarters building has been occupied for over a year but we don't yet "own the baby."

The only thing that has been asked of physicists and friends of physics is that they give a firm, decisive "Yes or No answer" to the question, "Will you help in the purchase of the Physics Headquarters Building?" and that a "Yes" answer be accompanied by a pledge or contribution. No firm of experts has been hired. No high powered methods have been used. A committee of physicists has done the work.

It has been hoped that practically all physicists and many friends of physics would make a contribution even though small. In some departments of Physics in universities there has been a 100 percent response, with graduate assistants necessarily giving small contributions. A large number of contributions of between one and ten dollars are needed as well as some more of the larger contributions from those who "have not yet got 'round to it."

The amount necessary for the purchase of the property and essential repairs is $81,000 of which $6000 remains to be subscribed by *individual physicists and friends of physics*. The amount needed for adapting the building to present needs and furnishing it is $30,000, of which $4000 remains to be contributed by industrial organizations interested in physics.

Frankly, I am proud of the fact that physicists and friends of physics have already raised over $100,000 to help promote the science of physics and thus show our interest and our faith in the future of our field. But I am disappointed in lack of response on the part of a large number. If you are one of these, I appeal to you to send a contribution, no matter how small, to the Headquarters Building Fund Committee, care of the American Institute of Physics, 57 East 55th Street, New York City, or to me at Norwich University, Northfield, Vermont.

If, by any chance, you are not familiar with the project, it is suggested that you refer to the Review of Scientific Instruments, August 1943, page 241; and the Journal of Applied Physics, September 1943, pages xi and xii, and October 1943, pages 499–509.

HOMER L. DODGE
Chairman, Building Fund Committee, American Institute of Physics

Here and There

Five Frank B. Jewett fellowships for research in the physical sciences have been awarded to Dr. Elliot R. Alexander, Dr. Albert S. Eisenstein, Dr. Kenneth Greisen, Dr. Boris Leaf, and Dr. Harry Pollard. Founded by the American Telephone and Telegraph Company, the fellowships are in honor of Frank B. Jewett, a vice president of that company who retired in 1944. Each fellowship is for one year and carries a stipend of $3000, with a further honorarium to the institution where the work is done. Primary criteria are: demonstrated research ability of the applicant, the fundamental importance of the problem he proposes to attack, and the likelihood of his growth as a scientist.

Science reports that the award for outstanding service to chemistry of the Pittsburgh Section of the American Chemical Society "for work worthy of note toward increasing chemical knowledge, promoting industry, benefiting humanity or advancing the Pittsburgh Section" was presented on February 15 to Dr. Leonard Harrison Cretcher, assistant director of the Mellon Institute and head of the department of research in pure chemistry.

The National Science Fund of the National Academy of Sciences has announced the creation of the "Charles L. Mayer Nature of Light Awards," two prizes of $2000 each, to be presented in 1946 for outstanding contributions to our knowledge of the nature of light. A detailed explanation may be obtained by writing to Howland H. Sargeant, Executive Secretary of the National Science Fund, at 2101 Constitution Avenue N. W., Washington 25, D. C.

A project in the form of an Award Program to encourage the preparation and publication of textbooks, one on machine design and another on structural design for fabrication by all processes, including welding, was recently announced by The James F. Lincoln Arc Welding Foundation, Cleveland, Ohio.

Said to be an important contribution toward stimulating instruction and study for engineering undergraduates in these important fields, the program will substantially reduce the usual delay between process developments in industry and the treatment of these new developments in textbook form. This is particularly significant in view of the many new applications and improvements in welding design techniques that have resulted from the intensified activity and advancements in arc welding during the past three wartime years. Thus the prime effect of the plan will be to render a service to engineering colleges and to the industries which employ their graduates by making this pertinent and timely information more conveniently available and comprehensible.

Further details of this new Award Program for textbooks, which closes May 15, 1946, may be obtained by addressing The Secretary of the Foundation at Cleveland 1, Ohio.

Ohmite Manufacturing Company has made an initial grant of $15,000 to Illinois Institute of Technology to be used for the establishment of a laboratory for the precision measurement of electrical and magnetic quantities. It represents the initial contribution for equipping what will be known as the Ohmite Laboratory for Precision Measurements, the ultimate goal of which is to provide precision electrical measurements for the Chicago area approaching in accuracy those of the Bureau of Standards in Washington, D. C. Working through the Armour Research Foundation, industries in the vicinity will have an opportunity to use the laboratory's facilities. This will be the first such laboratory in the Chicago area to make its services available to industry.

New Appointments

RCA Victor Division of Radio Corporation of America has announced the appointment of D. F. Schmit as Director of Engineering and George L. Beers as Assistant Director of Engineering.

John Vassos, designer, stylist, author, and illustrator, has resumed his association with the RCA Victor Division of Radio Corporation of America as consultant designer. He was recently honorably released from the Engineer Corps of the U. S. Army, where he attained the rank of Lieutenant Colonel, after two and one-half years of service on special missions in the European, African, and Middle Eastern war theaters.

New Booklets

The General Radio *Experimenter* is mailed without charge each month to engineers, scientists, technicians, and others interested in communication-frequency measurement and control problems. When sending request for subscription, give your name, company name and address, type of business the company is engaged in, and title of your position. Write to General Radio Company, 275 Massachusetts Avenue, Cambridge 39, Massachusetts.

A new 8-page condensed catalogue called *Norelco Electronic Products* has been announced by North American Philips Company, Inc., 100 East 42 Street, New York 17, New York. The subjects covered include cathode-ray tubes, oscillator plates, x-ray inspection units, x-ray spectrometer, x-ray diffraction equipment, x-ray analysis unit, metallurgical products, and medical x-ray equipment. Another recent publication of North American Philips is a 16-page illustrated booklet on *How and Why Cathode Ray Tubes Work*, including a discussion of complete television set-ups.

Scientific Electric, Division of "S" Corrugated Quenched Gap Company, has published *The ABC of Electronic Heating*, a 16-page booklet written for both engineer and manufacturer. It contains a brief record of the historical background and development of electronic heating, explains the principle of its operation, describes the two chief methods and fields of application, and lists many proved present-day uses. Many illustrations are used. Available upon request from Scientific Electric, 107 Monroe Street, Garfield, New Jersey.

Industrial Bulletin for February 1945, published by Arthur D. Little, Inc., of Cambridge, Massachusetts, features an article on modern methods of providing a fast, continuous bleaching of cotton and of synthetic fibers.

The Aerovox Research Worker, monthly house organ of the Aerovox Corporation, New Bedford, Massachusetts, "is published to bring to the radio experimenter and engineer authoritative, first-hand information on condensers and resistances for radio work." 50 cents per year in U.S.A., 60 cents per year in Canada.

Leaflets describing and cataloguing its line of laboratory apparatus and utensils made of Vitreosil (vitreous silica) are available from The Thermal Syndicate, Ltd., 12 East 46 Street, New York 17, New York. Equipment produced includes crucibles, dishes, muffles, pots, retorts, tanks, trays, tubes, pipes, and fittings.

Bakelite Review is published quarterly by Bakelite Corporation, unit of Union Carbide and Carbon Corporation, 30 East 42 Street, New York 17, New York, "to

inform industry of the latest developments in plastics and synthetic resins and their applications." The January 1945 issue, 28 pages, contains ten articles on present-day uses of plastics, particularly by the armed forces, and a "photo-story" on how the cross-sill of the Army wood truck body is made.

The Ohmite News for February featured a story of the building of the 200 kw shortwave transmitters constructed near Cincinnati to give the United States international broadcasting facilities equal to those of the Axis powers, for use in waging "psychological warfare." Address Ohmite Manufacturing Company, 4835 Flournoy Street, Chicago 44, Illinois.

Talk-A-Phone Manufacturing Company is offering a new and improved HP-16 Power Booster, which enables a regular inter-communication system to become a paging system also. For 8-page catalogue illustrating the Booster and its accessories, in addition to the complete Talk-A-Phone line of equipment, address the company at 1512 South Pulaski Road, Chicago 23, Illinois.

Leeds and Northrup Company have issued a revised edition of their earlier catalogue on white potentiometers. This may be of interest to any professors, laboratory instructors, and research and testing experts who do not have a copy of the original publication. Included is a complete description and diagram of the "single potentiometer" for measuring temperature with one thermocouple. Also featured is the "double potentiometer," which is equipped with two sets of dials so that thermocouples at different temperatures may be measured without resetting dials. Address Leeds and Northrup Company, 4934 Stenton Avenue, Philadelphia 44, Pennsylvania.

New Books

Proceedings of a Conference on Problems in the Utilization of Small Coals*

By British Coal Utilization Research Association, London. Pp. 294, Figs. 39, 14×22½ cm. Cheney & Sons, Banbury, England, 1944.

This book is a collection of 28 technical papers presented in 1943 before a conference led by the British Coal Utilization Research Association, the purpose being to discuss problems involved in burning the smaller sizes of solid fuels and the recovery of useful fuels from otherwise wasted colliery refuse. This means of extending England's dwindling wartime fuel supply was sufficiently interesting that some 700 persons attended the conference, including many government officials concerned with administering fuel supplies and persons having widest knowledge of fuel utilization problems. Thus it is evident that the information reported in these papers expresses the best now available in England on this subject. The fact that 25,000,000 tons of coal are produced annually in that country in sizes smaller than ¼-inch indicates the seriousness of the problem, particularly during wartime when every available ton of coal must be utilized. Likewise, when peace arrives, such information will be invaluable in improving the economic status of coal utilization by preventing needless waste of a useful product.

Problems associated with the burning of small fuels are discussed in the first eleven papers. These are not always clearly stated, however, and many of the papers wander into consideration of high ash content, excessive moisture, and similar factors, without limiting the discussion to size alone. It is obvious that some control of these variables is possible, whereas that of size is fixed and should have been of principal importance. In this connection, briquetting is mentioned so briefly as to approach complete disregard, probably for economic rather than technologic reasons. The ten papers following are devoted to small fuels having excessive ash content, interest being divided between problems involved in burning such fuels successfully and in means of recovering them. A great deal of emphasis is placed on the high ash content resulting from strip-mining operations, not because of the nature of the coal, but from poor mining practice. The last seven papers discuss the "up-grading" of fuels, in which particular attention is directed to removal of ash, reduction of moisture content, control of size, and blending. Most of the papers deal with "slurries," and the problems largely are those of the producer rather than the consumer.

Differences in nomenclature from those accepted in this country make parts of the book difficult for us to read; thus, reference to pearls, smalls, doubles, singles, or middlings will give the average American reader little information, although he may have some idea as to what is meant by duff or slurry. It would have been most helpful to have included, as an appendix, definitions of the more commonly used sizes of small coal in terms of dimensions, inasmuch as many of the authors neglected to specify the sizes of the coals they discussed except by name. It is suggested, since so much confusion in coal sizing still exists, that the conference could have achieved still greater benefits if one of its objectives had been standardization and definition of the size of small coals. As an illustration, the term "slurry" is used many times, but no less than six authors or discussors attempted to define it without reaching any general agreement.

A striking difference from the practice in this country is the quantity of small fuels apparently burned in hand-fired equipment. The use of pulverized coal is not extensive, the slag-tap furnace, for instance, being described as a sort of curiosity. Spreader stokers, called sprinkler-type stokers in England, are almost equally neglected, although one author describes a modern installation giving very satisfactory results with ¾-inch by zero slack. Burning of coke breeze and small coal on chain-grate stokers is covered adequately, the sandwich method commonly being used. Where coal alone is burned in the smallest sizes on these stokers, the difficulties are excessive, the fuel bed being unstable at normal burning rates so that there is considerable loss of fines to the flues. Installation of rakes to stir up the bed to prevent channeling is of no merit, but blending in the amount of 25 percent with larger fuels gives a sufficiently open bed to allow satisfactory rates of combustion.

Because most of the papers report the experiences of the authors and are thus factual, criticism of results usually is not warranted. However, in one case, where in discussing air supply to fuel beds, an author indicates furnace temperatures approaching 5000°F with 100 percent of normal air supply, some objection is justified. Obviously, he has become confused with theoretical flame temperature, but not even in this case can the temperatures be so high except with highly preheated air. Fortunately, no other errors of similar magnitude are apparent in the papers.

The book suffers from lack of editing, which would appear to be inevitable with any such compilation of papers prepared by a large number of authors acting individually. As a result, despite its division into three main sections, there is no clear-cut separation of subject matter, and the reader can study one phase completely only by scanning many others. This shortcoming is mitigated largely by an adequate subject index.

W. T. Reid
Bureau of Mines

* Published by permission of the Director, Bureau of Mines, U. S. Department of the Interior.

Letter to the Editor

Wave Equation for Finite Elastic Strains

A. NADAI
Westinghouse Research Laboratories, East Pittsburgh, Pennsylvania
(March 10, 1945)

MESSRS. B. A. Mrowca, S. L. Dart, and Eugene Guth described in a paper "Retraction and Stress Propagation in Natural and Synthetic Gum and Tread Stock" the results of a series of retraction tests with various rubber-like elastic materials. In these tests they recorded the elastic contraction of bars of such materials from a stretched condition after the tensile load had been suddenly released. They compared the results of their tests with the theory which was developed by Messrs. H. M. James and E. Guth in a note,[1] also recently published, for the propagation of an elastic impulse along such a specimen. In several figures of the first mentioned paper the authors reproduce elongation-time curves. Unit strains in these tests according to the curves reached values of the order of 100 percent. Despite the fact that the authors discuss cases in which a test specimen in its loaded condition was stretched to twice its original length and in which, therefore, the propagation of states of *elastic strains of a finite magnitude* was to be considered, they based their theoretical analysis on the classical equation of the longitudinal oscillations of an elastic bar *valid only for infinitesimal strains*. In their equation they included also a term for expressing internal damping. The equation which they used was:

$$\rho\frac{\partial^2 u}{\partial t^2}=f\frac{\partial^3 u}{\partial x^2\partial t}+E\frac{\partial^2 u}{\partial x^2} \tag{1}$$

(u displacement of a point, ρ density, E Young's modulus, f a damping constant, x coordinate, t time).

The purpose of this note is to develop an equation which, according to the opinion of this writer, should have been used when the laws for the propagation of an elastic state of strain of finite magnitude along a specimen was studied. With reference to Fig. 1 in which x and x'

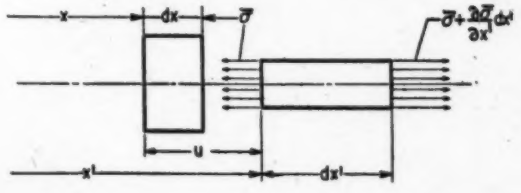

FIG. 1.

designate the coordinates of a material point of the bar in its original, unstressed, and in the strained condition, respectively, the equation of motion of an element of the bar is

$$\frac{\partial\bar\sigma}{\partial x'}-\rho\frac{\partial^2 x'}{\partial t^2}=0, \tag{2}$$

neglecting the effect of lateral accelerations in the bar and damping forces. Suppose also that the density ρ remains constant. In view of finite deformations use shall be made of the *natural strains* $\bar\epsilon$ defined by

$$\bar\epsilon=\ln(1+\epsilon). \tag{3}$$

ϵ designates the conventional strain in an element dx

$$\epsilon=(dx'-dx)/dx=\partial u/\partial x; \tag{4}$$

therefore

$$\bar\epsilon=\ln[1+(\partial u/\partial x)]. \tag{5}$$

Introducing "Hooke's law" for a hypothetic elastic material according to the equation:

$$\bar\epsilon=\bar\sigma/E, \tag{6}$$

where $\bar\sigma$ designates the *true* stress acting across a section of the bar in its deformed condition. For $\bar\sigma$ the expression

$$\bar\sigma=E\bar\epsilon=E\ln[1+(\partial u/\partial x)] \tag{7}$$

is obtained. Also

$$dx'=(1+\epsilon)dx=(1+\partial u/\partial x)dx. \tag{8}$$

Using Eqs. (7) and (8), Eq. (2) can be rewritten in either of the two forms:

$$\frac{\partial^2 u/\partial x^2}{(1+\partial u/\partial x)^2}=\frac{\rho}{E}\cdot\frac{\partial^2 u}{\partial t^2}\quad\text{or}\quad\frac{\partial}{\partial x}\left(\frac{1}{1+\partial u/\partial x}\right)+\frac{\rho}{E}\cdot\frac{\partial^2 u}{\partial t^2}=0. \tag{9}$$

A discussion of the propagation of impulses involving elastic strains of finite magnitude along a bar should have been based on Eq. (9). It can be seen that if the strain $\epsilon=\partial u/\partial x$ is equal to 1 (100 percent elongation) a factor equal to $\frac{1}{4}$ appears with which the term $\partial^2 u/\partial x^2$ has to be multiplied. For infinitesimal strains ϵ this factor would have been equal to 1. If internal damping forces of the usually assumed character shall also be considered, suppose that the true stress $\bar\sigma$ consists of two additive parts:

$$\bar\sigma=\bar\sigma'+\bar\sigma''. \tag{10}$$

Suppose that the first is the elastic stress $\bar\sigma'=E\bar\epsilon$ proportional to the natural strain $\bar\epsilon$ and that the second is proportional to the true (natural) rate of strain $\partial\bar\epsilon/\partial t$. We can write for

$$\bar\sigma=E[\bar\epsilon+t_0(\partial\bar\epsilon/\partial t)], \tag{11}$$

where t_0 is a material constant of the dimension of a time. Using the expression for $\bar\epsilon$ (Eq. (5)) the true rate of strain is found to be equal to

$$\frac{\partial\bar\epsilon}{\partial t}=\frac{\partial\epsilon/\partial t}{1+\epsilon}=\frac{\partial^2 u/\partial x\partial t}{1+\partial u/\partial x}. \tag{12}$$

For the equation of motion including internal damping

$$\frac{\partial^2 u/\partial x^2}{1+\partial u/\partial x}+t_0\frac{\partial}{\partial x}\left[\frac{\partial^2 u/\partial x\partial t}{1+\partial u/\partial x}\right]=\frac{\rho}{E}\left(1+\frac{\partial u}{\partial x}\right)\frac{\partial^2 u}{\partial t^2}, \tag{13}$$

is obtained instead of Eq. (1) proposed by the authors. Eq. (13) converges towards the simplified form of Eq. (1) considered by the authors if the strains ϵ remain infinitesimal.

[1] H. M. James and E. Guth, Phys. Rev. 66, 33 (1944).

Recent Applications of Physics

Prepared by CLARK GOODMAN, Associate Editor

Material to be included in this section should be submitted to Dr Clark Goodman, Massachusetts Institute of Technology, Cambridge 39, Massachusetts.

Bull's-Eye by X-Ray* Into the well-known picture of extremely high-voltage x-ray production have recently come two new tubes built for precision and enormous penetrating power. One, designed to operate on a direct-current potential of 2,000,000 volts, has been developed by the Machlett Laboratories, Inc.; the other, designed for alternating current of similarly great voltage, has been produced by the General Electric Company.

One of the major problems encountered in producing x-rays with very high voltages is that of confining the spot of impingement of electrons on the anode target to the smallest possible dimensions. If the electron beam diverges somewhat so that the spot is a quarter inch or so in diameter, as has usually been true, the x-rays struck off from the bombarded metal spread from an appreciable area, and vague edges on the shadow images in photographs result. Needed is a stream of x-rays emanating from a source as small as possible; hence the target spot affected by the electrons must be extremely small. The Machlett precision tube makes a notable advance in the attainment of this difficult requirement.

The method of focusing employed by the tube is somewhat analogous to that of an electron microscope. Essentially the tube is a 10-foot affair incorporating a five-foot column of metal and glass rings alternating with each other every half inch or so and sealed so perfectly that there are no leaks though the tube has 180 sections. Thus the interior can be exhausted and kept at a high vacuum for its entire life without an external pump; that is, the tube is sealed off like an ordinary radio tube. The cathode is a simple shielded tungsten filament. But at the anode end the target is something new—a disk of gold an inch and a quarter in diameter and a quarter of an inch thick. This gold also serves as the x-ray window, since the energy driven in line with the oncoming electrons passes through the gold and out at its farther side.

The tube is designed for operation under several hundred pounds of air pressure to give high insulation. The metal rings distribute the electric field so that an essentially even gradient exists from top to bottom. A narrow electron beam with little divergence is thus formed. As the electrons near the end of their run, they pass through a magnetic field lens which concentrates them so sharply that the target spot is smaller than the period at the end of this sentence. The x-ray emanation generated by this onslaught shoots principally downward in a narrow cone, with most of the intensity in the forward direction. The combination of magnetic lens arrangement and high voltage gives an efficiency on the order of 5 percent of the input energy.

This new weapon of the laboratory is an interesting example of what war necessity can do in applied technology. The average x-ray tube does not have more than two or three inches of metal-to-glass seals; this one has 300 feet, yet leaks give no trouble at all. The secret is in the method of building up the hollow column. This is done on a vertical revolving mandrel. A Pyrex glass ring and a Kovar alloy ring are laid one on top of the other on the mandrel, then heated with oxygen gas flames as they revolve, to give a rough joint. The area of contact of the two rings is thus filled with a thin layer of metallic oxide. When the bonding is good, the flames are turned off and the assembly is heated by a high-frequency coil which is lowered over it. The heating fuses the oxide layer and actually makes it flow into the glass so thoroughly that the molecules mingle and lock together. When this state has been reached all around the circumference and the pair of rings have been carefully centered, the mandrel is lowered slightly to bring them into an annealing chamber, the next pair of rings are added, and the fusing job is repeated. This process is continued until the whole tube is constructed.

Besides having applications in the war effort, the precision tube offers a tremendously powerful new means for further medical research, as well as an accurate source for x-ray photography both of tissues and of metals.

* This note was written by David O. Woodbury and is republished with the permission of the *Technology Review* in which it appeared in January, 1945.